Invent. math. 98, 445–489 (1989)

Inventiones mathematicae

Complex algebraic plane curves via their links at infinity

Walter D. Neumann
Department of Mathematics, Ohio State University, Columbus, OH 43210, USA

Summary. Considering that the study of plane cuves has an over 2000 year history and is the seed from which modern algebraic geometry grew, surprisingly little is known about the topology of affine algebraic plane curves. We topologically classify "regular" algebraic plane curves in complex affine 2-space using "splice diagrams:" certain decorated trees that code Puiseux data at infinity. (The regularity condition – that the curve be a "typical" fiber of its defining polynomial – can conjecturally be avoided.) We also show that the splice diagram determines such algebraic information as the minimal degree of the curve, even in the irregular case. Among other things, this enables algebraic classification of regular algebraic plane curves with given topology.

Let V be a reduced algebraic curve in $\mathbb{C}^2$. Then the intersection of V with any sufficiently large sphere S^3 about the origin in $\mathbb{C}^2$ is transverse, and gives a well-defined link (S^3, L), called the link at infinity of $V \subset \mathbb{C}^2$. The link at infinity is a useful tool for studying the topology of plane curves. In [N-R 1] this was illustrated by a quick uniform proof of the classification of polynomial injections of $\mathbb{C}$ in $\mathbb{C}^2$ due to Abhyankar and Moh [A-M 2] and Suzuki [S] in the smooth case and Zaidenberg and Lin [Z-L] in the non-smooth case. Here we develop the theory further.

We first recall some terminology and results from [N-R 1]. Let $f: \mathbb{C}^2 \to \mathbb{C}$ be a polynomial map. A fiber $f^{-1}(c)$ is called *regular* is nearby fibers "look like" $f^{-1}(c)$ in the sense that, for some neighborhood D of $c \in \mathbb{C}$, $f | f^{-1}(D)$: $f^{-1}(D) \to D$ is a locally trivial C^∞ fibration. The fiber $f^{-1}(c)$ is *regular at infinity* if nearby fibers "look like it at infinity;" that is, for some neighborhood D of c and some compact subset K of $\mathbb{C}^2$, $f | f^{-1}(D) - K$ is a locally trivial fibration. "Regular" is equivalent to "regular at infinity and non-singular".

Only finitely many fibers of f are irregular at infinity, and the regular fibers all define the same link at infinity up to isotopy, which we call the *regular link at infinity* of f and denote by $\mathscr{L}(f, \infty)$. If all fibers of f are regular at infinity we say f is *good*. This is so, for example, if any fiber of f is reduced

and has a knot as its link at infinity (i.e., it is connected at infinity), cf. [N-R 1, Lemma 7.1]. If f is good it is easy to see that there is a "Milnor fibration at infinity," so $\mathscr{L}(f, \infty)$ is a fibered link. The converse is true but less obvious: if f is not good then $\mathscr{L}(f, \infty)$ is not a fiberable link [N-R 1, Theorem 6.1]. One contribution of this paper is to provide a substitute for the Milnor fibration in this case.

An algebraic curve V will be called *regular* if it is a regular fiber of its defining polynomial f. A main result is that the link at infinity $\mathscr{L}=(S^3, L)$ of a regular algebraic curve $V \subset \mathbb{C}^2$ determines the topology of $V \subset \mathbb{C}^2$ (as an embedded C^∞ 2-manifold up to proper isotopy)[1]. In addition, even if V is not regular, it determines the euler characteristic of V (corrected by the Milnor numbers of the singularities of V if V is singular; Theorem 4.3), and also the degree and number of points at infinity of V in a sense that we now describe.

The degree $\deg(V)$ of V is only well defined relative to a fixed linear structure on $\mathbb{C}^2$; changing the embedding $V \subset \mathbb{C}^2$ by a non-linear automorphism[2] of $\mathbb{C}^2$ generally changes the degree (e.g. the curve $x^2+y^3=1$ of degree 3 is taken by the algebraic automorphism $(x,y) \mapsto (x+y^2, y)$ of $\mathbb{C}^2$ to the curve $(x+y^2)^2 + y^3 = 1$ of degree 4). Differently expressed, $\deg(V)$ depends on a choice of compactification $\mathbb{C}^2 \subset \mathbb{P}^2 = \mathbb{C}^2 \cup \mathbb{P}^1$: it is the algebraic intersection number with $\mathbb{P}^1$ of the closure $\bar{V}$ of V in $\mathbb{P}^2$. The number of points (as opposed to "places") at infinity $n_\infty(V) = |\bar{V} \cap \mathbb{P}^1|$ also depends on the compactification. We shall see that for a given V there are "minimal" embeddings $\mathbb{C}^2 \subset \mathbb{P}^2$ (characterized geometrically by the condition that either $n_\infty(V) > 1$ or $n_\infty(V) = 1$ and the first "Puiseux pair (p, q) at infinity" has $p, q > 1$) which lead to finitely many "minimal" choices for $(\deg, n_\infty)$—the choices with least $\deg(V)$ are among them. We shall see that these minimal pairs $(\deg, n_\infty)$ are simple invariants of the link at infinity[3]. We call the minimal value of deg and the maximal value of n_∞ for V the *intrinsic degree* and *intrinsic number of points at infinity* for V.

These results imply that for any given link $\mathscr{L}=(S^3, L)$ we can effectively decide if it is a link at infinity of some complex algebraic plane curve and, if so, write down the general polynomial that realizes it. But the calculation can be quite tedious already for simple examples. We thus do not yet have a complete "closed form" characterization of those links which can be realized as an $\mathscr{L}(f, \infty)$, but we have strong results towards it.

A corollary is a finiteness result (c.f. Corollary 8.2, which is sharper): there are only finitely many regular $V \subset \mathbb{C}^2$ up to smooth proper isotopy with given topology and with intrinsic number of points at infinity not 2. The exclusion of 2 intrinsic points at infinity is necessary: for $p, q > 0$ and coprime, the curve $x^p y^q = 1$ is an annulus in $\mathbb{C}^2$ whose link at infinity is a pair of parallel $(p, -q)$

---

[1] Conjecturally "regular" can be replaced by "nonsingular" here, see Sect. 9

[2] This does not change the link at infinity, cf. proof of Lemma 2.2 below

[3] For example, this least degree is p for the (p, q) torus knot with $1 < q < p$. Surprisingly, the least degree in which a link can be realized as a link of a singularity is *not* as simple an invariant of the link: this torus knot is realizable as a singularity link in degree approximately $\sqrt{pq}$ for p/q large; a degree 8 realization of the (29, 2) torus knot as a singularity link is $x^2+2xy^4+x^7y+y^8=0$ at (0, 0)

torus knots with opposing orientations; different pairs $\{p, q\}$ thus give non-isotopic annuli in $\mathbb{C}^2$.

Another application is to classifications of algebraic curves in $\mathbb{C}^2$ of low topological genus up to algebraic automorphisms of $\mathbb{C}^2$. For example, we immediately recover the Abhyankar-Moh Suzuki result that a smooth contractible algebraic curve in $\mathbb{C}^2$ is equivalent to the standard embedding of $\mathbb{C}$ in $\mathbb{C}^2$, but we easily get more: an algebraic embedding of $\mathbb{C}$ in $\mathbb{C}^2$ with one node is equivalent to the curve $y^2 = x^3 + x^2$; a smooth algebraic once punctured real torus in $\mathbb{C}^2$ is equivalent to a curve $y^2 = x^3 + ax + b$; a smooth algebraic once punctured genus 2 surface in $\mathbb{C}^2$ is equivalent to a curve $y^2 = x^5 + ax^3 + bx^2 + cx + d$; for genus 3 with one puncture there are 3 basic types, of intrinsic degrees 4, 6, and 7; for genus 4, 4 types, of intrinsic degrees 5, 6, 9, 9, and so on. We can also describe all regular algebraic annuli in $\mathbb{C}^2$ up to algebraic automorphisms[4]: for each coprime positive integer pair (p, q) there is a family containing the example $x^p y^q = 1$ of the previous paragraph (Proposition 8.4).

We now describe our main results in more detail.

Theorem 1. *The topology of a regular algebraic plane curve $V \subset \mathbb{C}^2$ (as an embedded smooth manifold) is determined by its link $\mathscr{L} = (S^3, L)$ at infinity. In fact a minimal Seifert surface F for L in S^3 is unique up to isotopy[5] in S^3, and V can be recovered up to proper isotopy by attaching a collar out to infinity in $\mathbb{C}^2$ to the boundary of such an F.*

A link at infinity is always a *toral link*, that is, it can be built up by iterated cabling operations from the unknot. In [E-N] such links are classified by *splice diagrams*. To describe our next main result we need a quick review of splice diagrams for toral links; more details are given in Sect. 3.

We must first fix terminology about cabling. Given a component K of a link $\mathscr{L} = (S^3, L)$, let $N(K)$ denote any closed solid torus neighborhood of K which is disjoint from all other components of L. An (α, β) *cable* on K is a simple closed curve $K(\alpha, \beta)$ which lies on some $\partial N(K)$ and is homologous in $N(K)$ to αK and has linking number β with K (so α and β must be coprime). Several (α, β) cables on K are *parallel* if they lie on some common $\partial N(K)$ and are mutually disjoint. An (α, β) *cabling operation on the component K of $\mathscr{L}$* is the operation of either replacing K by, or adding, some number $d \geqq 1$ of parallel (α, β) cables on K, to obtain a new link (our terminology differs from [E-N], where this is called $(d\alpha, d\beta)$ cabling).

Splice diagrams are certain decorated trees used to represent toral links. The "decorations" consist of integer weights at the ends of some edges. Also, some of the vertices are drawn as arrowheads; they correspond to components of the link. When constructing a toral link by iterated cabling, we may start from the "n-component Hopf link" $\mathscr{H}_n = (S^3, K_1 \cup \ldots \cup K_n)$ consisting of n fibers of the Hopf fibration. We represent this link by the splice diagram with n arrowheads:

---

[4] Irregular algebraic annuli exist and are not yet classified – see Sect. 8

[5] A minimal Seifert surface F is a surface with maximal euler characteristic among all oriented embedded surfaces with no closed components in S^3 with $\partial F = L$. F may not be unique up to isotopy as a Siefert surface: the isotopy need not fix L

If $n=1$ or 2 this diagram may be abbreviated to $\circ\!\!\rightarrow$ or $\longleftrightarrow$ respectively, but we will not always want to do this.

If $\boxed{\Gamma}\!\!\rightarrow$ is a splice diagram for a link $\mathscr{L}$ and the indicated arrowhead corresponds to a component K, then each of the diagrams

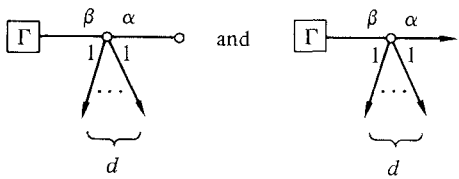

represents the result of doing an (α, β) cabling operation to $\mathscr{L}$; namely, either replacing component K by, or adding, d parallel (α, β) cables on K. One can thus construct a splice diagram for any toral link. In [E-N] it is shown that the splice diagram determines the link. The splice diagram itself is determined by the link only up to certain operations which we recall in Sect. 3; for instance, an edge with weight 1 at one end and a leaf[6] at its other end can be discarded; vertices of valency 2 can be ignored; also certain changes of sign of the weights in a splice diagram are allowed.

If we have constructed a toral link by iterated cabling from $\mathscr{H}_n$ then we call the vertex of its splice diagram which comes from this $\mathscr{H}_n$ the *root vertex* of the splice diagram and speak of a *rooted splice diagram.* There may be many ways of picking a root vertex in a splice diagram for a toral link; they represent different ways of constructing the link by iterated cabling. For example, the following rooted diagrams give 2 different constructions for one link; the root vertex is marked as a "●" in each:

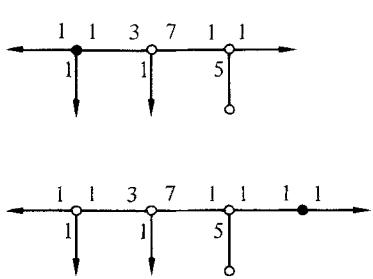

In the first case we start from $\mathscr{H}_3=(S^3, K_1\cup K_2\cup K_3)$ and add a (7, 3) cable $K_3(7, 3)$ and then replace K_3 by its (5, 1) cable $K_3(5, 1)$. In the second case we start from $\mathscr{H}_2$, add the (5, 1) cable $L=K_2(5, 1)$, and then successively add $L(3, 7)$ and $L(1, 1)$ (note that $L(1, 1)$ is drawn on the boundary of a "thinner" solid torus than $L(3, 7)$, since the solid torus must be disjoint from the already existing $L(3, 7)$).

[6] A leaf is a non-arrowhead vertex of valency 1 – valency is number of incident edges at the vertex

In a rooted splice diagram we call a weight on an edge *near* or *far* according as it is on the end of the edge nearest to or farthest from the root vertex. At most one near weight at any vertex is unequal to 1. (Splice diagrams which admit no root vertex satisfying this constraint also have meaning but are not important here: they represent links in homology spheres which may not be S^3.)

We shall say a cabling construction of a link $\mathscr{L}$, starting from an n-component Hopf link $\mathscr{H}_n$, satisfies *reverse Puiseux inequalities* if the following four conditions are satisfied:

(i) the cabling coefficients (α, β) always have $\alpha > 0$;

(ii) the first cabling done on each K_i has $\beta - \alpha < 0$;

(iii) any (α, β) cabling on some component following a (γ, δ) cabling on the same component has $\beta\gamma - \alpha\delta < 0$;

(iv) any (α, β) cabling on a component that was obtained by an (γ, δ) cabling operation has $\beta - \gamma\delta\alpha < 0$.

In terms of the rooted splice diagram these conditions can be more briefly stated:

(i) all near weights are positive;

(ii–iv) for any edge with weights α_0 and α_1 on it and weights $\alpha_2, \ldots, \alpha_m$ adjacent to but not on it,

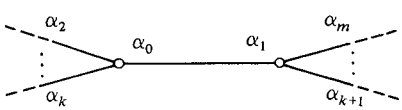

one has $\alpha_0\alpha_1 - \alpha_2 \ldots \alpha_m < 0$, that is, the "*edge determinant*" is negative.

(The *Puiseux inequalities*, which are necessary and sufficient conditions for a link to be a link of a plane curve singularity, are equivalent to requiring that the link have a construction satisfying (i) together with the reverse inequalities of (ii), (iii), (iv). In terms of a splice diagram this says simply that all weights and all edge determinants are positive.)

A construction satisfying the reverse Puiseux inequalities will be called *an RPI construction* and the corresponding rooted splice diagram will be called an *RPI splice diagram.* Given such a construction for a link $\mathscr{L} = (S^3, L)$, we can redo the construction of $\mathscr{L}$ to create extra components (which are never themselves cabled on) as follows: start from $\mathscr{H}_{n+1} = (S^3, K_0 \cup K_1 \cup \ldots \cup K_n)$ instead of $\mathscr{H}_n$ (so K_0 is an extra component) and, whenever a cabling operation is performed, include an extra parallel cable (which is never cabled on later). The extra components created this way will be called *virtual components of the first kind* for the construction. Any K which was replaced in some cabling operation during the construction is called a *virtual component of the second kind.* These virtual components can be associated in a natural way with the non-arrowhead vertices in the splice diagram. In particular, K_0 is the virtual

component for the root vertex. We shall denote the virtual component corresponding to a vertex v by S_v and denote by $l_v = \text{link}(S_v, L)$ the linking number of this virtual component with the link. A quick way of computing these linking numbers from the splice diagram is quoted in Lemma 3.2.

An RPI splice diagram for which the above l_v are all non-negative will be called a *regular splice diagram.* A link which has a regular splice diagram will be called a *regular toral link.* It is sufficient for regularity that the conditions $l_v \geqq 0$ hold for each virtual component of the first kind parallel to a link component (i.e. v is a node adjacent to an arrowhead), see Corollary 5.2. It also follows from Sect. 6 that if some RPI splice diagram for a link $\mathscr{L}$ is regular then every RPI splice diagram for $\mathscr{L}$ is regular.

Theorem 2. (i) *A reduced algebraic curve $V \subset \mathbb{C}^2$ together with a chosen embedding $\mathbb{C}^2 \subset \mathbb{P}^2$ determines an* RPI *splice diagram Ω for the link at infinity of V. The number of points at infinity $n_\infty(V)$ is the valency n of the root vertex in Ω and $\deg(V)$ is the linking number l_{root} of the virtual component for the root vertex with the link. If V is a regular curve then Ω is a regular splice diagram.*

(ii) *A link is a sublink of some link at infinity (which can be chosen regular, or even good) if and only if it has an* RPI *splice diagram.*

An RPI construction for a link $\mathscr{L}$ may involve unnecessary cabling operations which just replace a curve by an isotopic curve, but there are finitely many *minimal* RPI constructions, described by *minimal RPI splice diagrams*, which involve no such cablings. An embedding $\mathbb{C}^2 \subset \mathbb{P}^2$ is, by definition, *minimal for V* in the sense described earlier if and only if the corresponding RPI splice diagram is minimal. A regular toral *knot* has just one minimal RPI splice diagram. Explicit general bounds on the number of minimal RPI splice diagrams are given by Theorems 6.2 and 6.5, the essential point being that *for a link of interest to us, minimal RPI diagrams can differ only in the position of the root vertex.* Using this, we show:

Theorem 3. *For a reduced algebraic curve $V \subset \mathbb{C}^2$, every minimal* RPI *splice diagram for its link at infinity is realized by an embedding $\mathbb{C}^2 \subset \mathbb{P}^2$. In particular, any pair $(\deg(V), n_\infty(V))$ for V which either minimizes $\deg(V)$ or has $n_\infty > 1$ equals the degree and number of points at infinity determined by some minimal* RPI *splice diagram for its link at infinity.*

If V is connected at infinity, the above theorem is implicit, in quite different language, in the paper of Abhyankar and Singh [A-S].

Some of the topological ingredients in this paper have independent interest. One ingredient for Theorem 2 is a computation in terms of splice diagrams of the effect of Dehn surgery on a component of a toral link. We describe this in Sect. 3 in the greater generality of "graph links" since it is of wider use and involves little extra work.

Theorem 1 follows from the next two results.

Theorem 4. (i) *A regular plane curve V can be recovered up to proper isotopy from a suitable spanning surface $F \subset S^3$ for its link at infinity $\mathscr{L} = (S^3, L)$ by attaching a collar out to infinity in $\mathbb{C}^2$ to the boundary ∂F.*

(ii) *F is the fiber of some fibered multilink with positive multiplicities.*

A multilink, see below or [E-N], is a link whose components have been assigned integer multiplicities; it is fibered if its exterior—the complement of an open tubular neighborhood of the link—is fibered over the circle by a map whose degree on any curve is the linking number of the curve with the link, taking multiplicities into account.

If the defining polynomial $f\colon \mathbb{C}^2 \to \mathbb{C}$ for V is good then, as already mentioned, $\mathscr{L}$ has a "Milnor fibration," and in this case Theorem 1 is easy: $F \subset S^3$ is a fiber for the link, and the fact that a minimal Seifert surface for a fibered link is unique up to isotopy and isotopic to a fiber is proved in [E-N, Sect. 4]. In general, given Theorem 4, Theorem 1 is a special case of the following more general result about fibered multilinks in homology spheres:

Theorem 5. *If a fibered multilink in a homology sphere Σ has no component of multiplicity zero then the boundary of a fiber F for the multilink determines the multilink and its fibration up to isotopy. Moreover, any minimal Seifert surface for the link $(\Sigma, \partial F)$ is isotopic to F (the isotopy may not fix ∂F)*[7].

Note that Theorem 5 implies that the multilink associated to a non-fiberable regular link at infinity is unique up to isotopy. The relationship of this multilink with the defining polynomial f can be quite subtle. The following example seems fairly typical. More examples and discussion are in Sects. 8 and 9.

Example[8]. Consider $f(x, y) = x^p y^q + y$ with $gcd(p, q) = gcd(p, q-1) = 1$, $p > 1$, $q > 1$. The only irregular fiber is $f^{-1}(0)$. The regular fiber is a twice punctured surface of genus $(p-1)/2$. Its link at infinity has RPI splice diagram

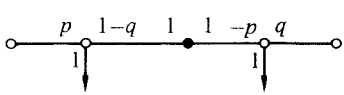

In the RPI construction of $\mathscr{L}$, the curves $x=0$ and $y=0$ play the roles of K_1 and K_2 (the virtual component K_0 can be represented for example by $x+y=0$) and the two components are a $(p, 1-q)$ cable on K_1 and a $(q, -p)$ cable on K_2. The multilink corresponding to $\mathscr{L}$ has diagram

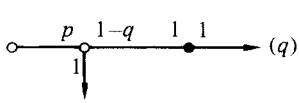

where the q in parentheses indicates that the component K_2 has multiplicity q. It is not hard to show that the underlying link $L_1 \cup K_2$ of this multilink is not realizable as a link at infinity, however one orients its components, if

[7] This is a special property of such a link: a general link may have many non-diffeomorphic minimal Seifert surfaces

[8] This example answers the question of [S, p. 250] negatively

$q>2$. Finally, the irregular fiber $f^{-1}(0)$ is the disjoint union of an annulus and a disk; its link at infinity has splice diagram

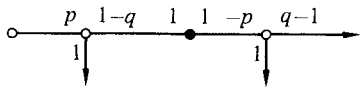

The computation of such examples is not hard: compute the splice diagrams for the links of the singularities on $\mathbb{P}^1$ of $\bar{V} \cup \mathbb{P}^1 \subset \mathbb{P}^2$ (this is the same as computing the Newton-Puiseux pairs, for which there are standard techniques); the desired RPI splice diagram then results by an easy manipulation described in Sect. 4.

Acknowledgements. Conversations with Lee Rudolph have been very helpful. The support of the N.S.F. for this work is gratefully acknowledged. The research for this paper was started while the author was enjoying the hospitality of the Max-Planck-Institut für Mathematik in Bonn.

1. Proof of Theorem 5: fiber boundaries of multilinks

Recall (cf. [E-N]) that a *multilink* in a homology 3-sphere Σ consists of an oriented link $\mathscr{L}=(\Sigma, L)$ (so L consists of a disjoint collection of smoothly embedded oriented circles in Σ) together with an integer "multiplicity" assigned to each component K_i of L with the convention that a component K_i with multiplicity m_i is considered equivalent to $-K_i$ (that is K_i with reversed orientation) with multiplicity $-m_i$. Such a multilink has a unique-up-to-homotopy map π: $E(L) \to S^1$ of its *exterior* $\mathrm{E(L)}=\Sigma-\mathrm{int}\, N(L)$ to S^1 ($N(L)$ denotes a closed tubular neighborhood of L in Σ) whose degree on any closed curve in $E(L)$ is the linking number of the curve with L, taking multiplicities into account. Conversely, any homotopy class of maps π: $E(L) \to S^1$ determines a multilink structure on $\mathscr{L}$. If this homotopy class contains a fibration, the multilink is said to be fiberable and $\mathscr{L}$ plus such a fibration is called a *fibered multilink*. In [E-N, Sect. 4] it is shown that the fibration of a fiberable multilink is unique up to isotopy. Since $[E(L), S^1]=H^1(E(L); \mathbb{Z})$ canonically, the homotopy class $[\pi]$ determines an element of $H^1(E(L); \mathbb{Z})$, which we call the *multiplicity class* for $\mathscr{L}$. It is dual to the homology class in $H_2(E(L), \partial E(L); \mathbb{Z})$ represented by any Seifert surface for the multilink.

A *fibered link* is the special case of a fibered multilink with all multiplicities equal to ± 1. We can choose the component orientations so that the multiplicities are all $+1$. In this case L is isotopic, as an oriented link, to the boundary ∂F of a fiber F of the fibration. However, if $\mathscr{L}$ is a fibered multilink whose component multiplicities are not all ± 1 then the boundary ∂F of a fiber will be some cabling of L. Theorem 5 says that $\mathscr{L}=(\Sigma, L)$ can nevertheless be recovered, as a multilink, from the oriented link $\mathscr{L}'=(\Sigma, \partial F)$, so long as no component of $\mathscr{L}$ has multiplicity zero. To prove this we must recognize whether a compo-

nent K_0 of ∂F which is a non-trivial cable arises in ∂F because K_0 itself occurs (up to isotopy) as a component of $\mathscr{L}$, or because the curve K that it is a cable on occurs as a (multiple) component of $\mathscr{L}$. As we shall see, K is a component of $\mathscr{L}$ if and only if "K_0 contributes to the non-fiberability of $\mathscr{L}'=(\Sigma, \partial F)$."

Proof of Theorem 5. Note first that a fibered multilink is irreducible (also called "non-split"), that is, the link exterior $E(L)$ is irreducible: it contains no embedded 2-spheres which do not bound balls. As described in [E-N], the toral decomposition theorem of Jaco-Shalen [J-S] and Johannson [J], applied to the irreducible link exterior $E(L)$ of $\mathscr{L}$, gives the *minimal splice decomposition* for the multilink $\mathscr{L}$. Namely, $E(L)$ is written as the union of pieces E_j pasted together along torus boundary components, these tori are incompressible and non-boundary-parallel in $E(L)$, each E_j is either simple or Seifert fibered, and Seifert fibrations on adjacent E_j's can never be made to agree along their common torus (this latter condition gives the minimality of the decomposition). Each E_j is itself a multilink exterior: $\Sigma - \text{int } E_j$ is a disjoint union of homology solid tori and replacing each of them by a homologically equivalent genuine solid torus gives a homology sphere Σ_j, the cores of these solid tori form a link L_j and Σ_j, and the multilink structure is determined by the restriction $\pi_j = \pi | E_j$ of the map π: $E(L) \to S^1$ which gives the multilink structure of $\mathscr{L}$. In [E-N, Theorem 4.2] it is shown that $\mathscr{L}$ is fiberable if and only if each of the *splice components* $\mathscr{L}_j=(\Sigma_j, L_j)$ is fiberable, that is, each π_j is homotopic to a fibration.

Now let $\mathscr{L}=(\Sigma, L)$ be a fibered multilink with no component of multiplicity zero. We shall choose orientations so that all multiplicities are positive. Let $\mathscr{L}'=(\Sigma, \partial F)$. If $\mathscr{L}$ is a link, that is, all multiplicities are 1, then $\mathscr{L}' \cong \mathscr{L}$, so in particular $\mathscr{L}'$ is a fibered link. On the other hand, if $\mathscr{L}$ is not a link, that is, some multiplicity is >1, then we shall see below that $\mathscr{L}'$ is not a fibered link. Thus $\mathscr{L}'$ detects whether $\mathscr{L}$ is a link, and in case $\mathscr{L}$ is a link the Theorem is just reiterating the results already quoted, that the fibration of a fibered link is unique up to isotopy and any minimal Seifert surface is isotopic to a fiber. We will therefore assume from now on that some multiplicity is >1.

Suppose next that the underlying link without multiplicities is either the unknot in S^3 or the *positive or negative Hopf link* (two unknotted circles in S^3 linking once with linking number $+1$ or -1). For the unknot with multiplicity $p>1$ the fiber F is p disks and ∂F is the reducible link consisting of p unknotted unlinked circles. For the positive or negative Hopf link with multiplicities p and q the fiber F consists of $d=GCD(p, q)$ annuli connecting pairs of parallel $(p/d, \pm q/d)$ torus knots and ∂F consists of the $(2p, \pm 2q)$ torus link with d of its $2d$ components reversed in orientation (in particular $\mathscr{L}'$ has just one splice component). In each of these cases it is easy to see that $\mathscr{L}'$ is nonfiberable (see [E-N, proof of 11.2). The following Lemma shows that we can recognize from $\mathscr{L}'$ whether we are in one of these cases. Theorem 5 is then easily verified for them.

Assume now that $\mathscr{L}$ is not as above. We shall show:

Lemma 1.1. (i) *$\mathscr{L}'$ is distinguished from the previous cases in that it is non-fiberable, irreducible, and has more than one splice component in its minimal splice decomposition.*

(ii) *Each non-fiberable splice component in the minimal splice decomposition of $\mathscr{L}'$ has Seifert fibered exterior with a single multiple fiber. To recover $\mathscr{L}$ from $\mathscr{L}'$, replace the part K_0 of ∂F occurring in each such splice component by the corresponding multiple fiber K of the Seifert fibration and give K the orientation and multiplicity that makes it homologous to K_0 in a neighborhood of K (this is its multiplicity as a Seifert fiber).*

Proof. If K is a component of our fibered multilink $\mathscr{L}$ of multiplicity 1 then the corresponding portion of ∂F is just a parallel copy of K. On the other hand, if K is a component of multiplicity $p>1$, then the corresponding part K_0 of ∂F is a d-fold $(p/d, q/d)$-cable on K for some q, where $d=gcd(p, q)$ (cf. [E-N, p. 29]). As described in [E-N, Proposition 1.1] (see also Sect. 3), such a cabling corresponds to adding a splice component to $\mathscr{L}$. The exterior E for this splice component is $E=N(K)-\text{int } N(K_0)$, where $N(K)$ and $N(K_0)$ are suitable tubular neighborhoods of K and K_0 with $N(K_0)\subset \text{int } N(K)$. This E is Seifert fibered with typical fibers being parallel to the components of K_0 and with K as the unique singular fiber. Let us call such a splice component of $\mathscr{L}'=(\Sigma, \partial F)$ a "new" splice component. We splice decompose $\mathscr{L}'$ by taking a minimal splice decomposition of $\mathscr{L}$ and adding the new splice components. The splice components that come from $\mathscr{L}$ we call "old".

Since F is a Seifert surface for $\mathscr{L}'$, it is dual to the multiplicity class for $\mathscr{L}'$. It is of course also dual to the multiplicity class for $\mathscr{L}$. In particular, the old splice components of $\mathscr{L}'$ agree as *multilinks* with the corresponding splice components of $\mathscr{L}$, and are hence fiberable. On the other hand, F has intersection number 0 with the Seifert fibers in each new splice component exterior, so by [E-N, Theorem 11.2], these are not fiberable multilinks.

The above splice decomposition of $\mathscr{L}'$ is minimal. Indeed, suppose an old splice component exterior adjacent to a new splice component exterior is also Seifert fibered; we must show that the Seifert fibrations do not agree up to homotopy along the common torus. But if they did, then F would have intersection number 0 with the fibers of this old splice component, contradicting the fiberability of $\mathscr{L}$. (This argument does not apply when the underlying link of $\mathscr{L}$ is the unknot or a Hopf link – excluded in the Lemma. These might be thought of as the cases where $\mathscr{L}$ has "no" splice components.)

Since some multiplicity in $\mathscr{L}$ is >1, there is at least one new splice component in $\mathscr{L}'$. Thus $\mathscr{L}'$ is not fiberable, and its minimal splice decomposition has at least two splice components. The existence of a minimal splice decomposition implies the irreducibility of $\mathscr{L}'$. Finally, part (ii) of the Lemma follows from our description of the new splice components. □

The first sentence of Theorem 5 is proved. We must still show that, if $\mathscr{L}$ is as in the above Lemma, any minimal Seifert surface F' for $\mathscr{L}'$ is isotopic to F. Any minimal Seifert surface for an irreducible multilink can be isotoped to intersect each splice component in a minimal Seifert surface for that splice component (cf. [E-N, Theorem 3.3]; isotopy is not claimed there, but the proof easily yields it); moreover, a minimal Seifert surface in a fibered multilink is isotopic modulo boundary to a fiber [E-N, Proposition 4.1]. Thus F' can be assumed to equal F outside the new splice components. Denote this part of

F and F' by F_0. The part $F - \operatorname{int} F_0$ of F inside the new splice components is a union of annular collars on boundary components of F. The same must be true for F', since anything else would decrease the euler number and contradict minimality. Thus F' and F are both isotopic to F_0 and hence to each other. □

For convenience we record here the following.

Proposition 1.2. *If a fibered multilink $\mathscr{L}$ has at least one component of multiplicity $\neq \pm 1$, then the link $\mathscr{L}'$ given by a fiber boundary for $\mathscr{L}$ is not fiberable.*

Proof. If no component has multiplicity 0 this is a corollary of Theorem 5 (and an ingredient in its above proof). If a component does have multiplicity 0 then $\mathscr{L}'$ is reducible and hence not fiberable. □

2. Proof of Theorem 4: the multilink associated with a link at infinity

We first describe why a regular complex algebraic curve $V \subset \mathbb{C}^2$ can be recovered up to proper isotopy from a spanning surface F for the link at infinity $\mathscr{L} = (S^3, L)$. Let $f: \mathbb{C}^2 \to \mathbb{C}$ be a defining polynomial for V. Let n be the degree of f. By a linear change of coordinates $(x, y) \in \mathbb{C}^2$ we can put $f(x, y)$ in the form

$$f(x, y) = x^n + f_{n-1}(y)\, x^{n-1} + \ldots + f_0(y).$$

Since f has only finitely many irregular fibers (this follows from the proof of the next lemma), their images will all be contained in the interior of some sufficiently large disk $D^2(s) = \{z \in \mathbb{C} \mid |z| \leqq s\}$ about the origin $0 \in \mathbb{C}$. Consider the polydisk $D(q, r) = \{(x, y) \in \mathbb{C}^2 \mid |x| \leqq q, |y| \leqq r\}$.

Lemma 2.1. *For s as above sufficiently large, r sufficiently large with respect to s, and q sufficiently large with respect to r and s, the fibers $f^{-1}(z)$ for $z \in \partial D^2(s)$ intersect $\partial D(q, r)$ only in the part $|x| < q$, $|y| = r$, and do so transversely — in fact, they intersect each line $y = y_0$ with $|y_0| = r$ transversely.*

Proof. If, for given r and s, $f^{-1}(D^2(s))$ intersected $\{|x| = q, |y| \leqq r\}$ non-trivially for arbitrarily large q, then $y = 0$ would be a point at infinity of the fibers $f^{-1}(z)$. This is not so, so for large q, $f^{-1}(D^2(s))$ only meets the other part $\{|x| < q, |y| = r\}$ of $\partial D(q, r)$.

To see the transversality statement, consider $f(x, y) - z$ as a polynomial in x with coefficients in $\mathbb{C}[y, z]$ and form its discriminant $\Delta \in \mathbb{C}[y, z]$. (Recall that the discriminant of a degree n polynomial $f \in R[x]$ over a ring R is $\Delta = \prod_{i<j} (\xi_i - \xi_j)^2$, where the ξ_i, $i = 1, \ldots, n$, are the formal roots of $f = 0$; it is a polynomial in the coefficients of f and it vanishes if and only if $f = 0$ has multiple roots.) Then the fiber $f^{-1}(z_0)$ is transverse to the line $y = y_0$ if and only if $\Delta(y_0, z_0) \neq 0$. In particular, the fiber $f^{-1}(z_0)$ is regular at infinity if $\Delta(y, z) \neq 0$ for each z close to z_0 and each y of sufficiently large absolute value. But this fails if and only if $z = z_0$ is tangent to $\Delta(y, z)$ at infinity. In homogeneous coordinates (y, z, w)

at infinity, this says that $z=w=0$ is a point of $\Delta=0$ and $z=z_0 w$ is a tangent line to $\Delta=0$ at this point. This can only happen for finitely many z_0, so we choose our disk $D^2(s)$ to contain these values in its interior. □

Now choose q, r, and s, as in the above Lemma.

Lemma 2.2. *$D=f^{-1}(D^2(s))\cap D(q,r)$ is a 4-disk with piecewise-smooth boundary which decomposes as $\partial D=S\cup E$ with*

$$S=\partial D(q,r)\cap f^{-1}(D^2(s)),$$

$$E=D(q,r)\cap\partial(f^{-1}(D^2(s))),$$

and f restricts to a fibration of E over a circle and a typical fiber $F=f^{-1}(z)\cap E$ of $f|E$ satisfies:

(i) *$f^{-1}(z)-\operatorname{int} F$ is a collar out to infinity on ∂F;*

(ii) *the pair $(\partial D, \partial F)$ is equivalent to the link at infinity (after smoothing the corner along $\partial S=\partial E$).*

Proof. One can follow the standard model for such proofs, Milnor's proof [M] that the link of an isolated critical point is fibered: by mirroring his proof one can construct a suitable vector field along which to isotop the one construction to the other. We give a modified argument which shows that any two reasonable constructions of a "link at infinity" give the same answer. In particular, a change of coordinates in $\mathbb{C}^2$ does not change the link at infinity, a fact that we have been implicitely assuming but which requires proof.

We shall call a manifold pair (Σ, L) an *abstract link at infinity* for $(\mathbb{C}^2, V)$ if $(\Sigma, L)\times[0,\infty)$ is diffeomorphic to a neighborhood of infinity for the pair $(\mathbb{C}^2, V)$. We first note that any two abstract links at infinity for $(\mathbb{C}^2, V)$ are diffeomorphic, since they are homotopy equivalent as pairs, so one can apply Waldhausen [W].

To see that $(\mathbb{C}^2-\operatorname{int}(D), f^{-1}(z)-\operatorname{int}(F))$ is homeomorphic (diffeomorphic after smoothing corners) to $(\partial D, \partial F)\times[0,\infty)$ as desired, integrate along a suitable smooth vectorfield v on $\mathbb{C}^2-\operatorname{int}(D)$ which is transversal inward on ∂D, is tangent to the fibers $f^{-1}(z)$ for $|y|\geqq r$ and $z\in\partial D^2(s)$, and whose v-derivative satisfies the following for some small ε: $v(|y|^2)\leqq -1$ when $|y|\geqq r-\varepsilon$ and $|f(x,y)|\leqq s+\varepsilon$, and $v(|f(x,y)|^2)\leqq -1$ otherwise. Such a vectorfield is easily constructed locally using the lemma, and a partition of unity then does it globally. □

To complete the proof of Theorem 4 (and hence also Theorem 1) we must show that F is a fiber of a multilink with no zero multiplicities. I am grateful to Lee Rudolph for the following very simple proof of this fact. It is also a consequence of Theorem 2 and its proof, as we describe later (Remark 4.1 and Corollary 5.3).

We want to show that S is a union of solid tori, to exhibit F as a fiber of a multilink structure on the link consisting of the cores of these solid tori. Note that for $|y_0|=r$ the intersection $S_0=\{(x,y)|y=y_0\}\cap f^{-1}(D^2(s))$ is transverse. Moreover, S_0 is equivalent to the set $\{x\in\mathbb{C}\,|\,\|f(x,y_0)\|\leqq s\}$, which is a

collection of disks, since it is bounded and its complement in $\mathbb{C}$ can have no bounded components (such components would contradict the maximum modulus principle). It follows that S consists of solid tori as claimed, so we have constructed the desired multilink.

The transversality of the intersection $\{(x, y)|y=y_0\} \cap f^{-1}(z)$ also shows that $\partial F = S \cap f^{-1}(z)$ intersects each S_0 transversely, so every component of our multilink has nonzero multiplicity. Theorem 1 now follows from Theorem 5. □

Remark 2.3. The results of [N-R 1] quoted in the Introduction follow easily by the present approach. We sketch the proofs.

If f is not good then $\mathscr{L}(f, \infty)$ is not fiberable. Proof. If f is not good then, with notation as above, $f|S_0$: $S_0 \to D^2$ has non-empty branch set (there is a branch point near any fiber which is irregular at infinity). Thus the multilink associated to $\mathscr{L}(f, \infty)$ has at least one component of multiplicity >1, so $\mathscr{L}(f, \infty)$ is not fiberable by Proposition 1.2. □

If $V=f^{-1}(0)$ is reduced and connected at infinity then f is good. Proof. The link at infinity of V is homologous in S to the associated multilink, so the multilink has only one component[9]. That is, it is a fibered knot with multiplicity. Call the multiplicity m. We must show $m=1$. The general fiber of f has m components, so f can be factored as $g \circ f_0$ for some polynomials f_0: $\mathbb{C}^2 \to \mathbb{C}$ and g: $\mathbb{C} \to \mathbb{C}$, with g of degree m. Since f has a reduced and connected fiber, $m=1$. □

3. Splice diagrams and Dehn surgery

We first recall here, as briefly as possible, what we need of the language of splice diagrams. See [E-N] for more details.

Given links in homology spheres $\mathscr{L}'=(\Sigma', L')$ and $\mathscr{L}''=(\Sigma'', L'')$ and components $K' \subset L'$ and $K'' \subset L''$, the *splice $\mathscr{L}=(\Sigma, L)$ of $\mathscr{L}'$ and $\mathscr{L}''$ along K' and K''* is constructed as follows. Σ is obtained by pasting together complements of open tubular neighborhoods of K' and K'': $\Sigma=(\Sigma'-N(K')) \cup (\Sigma''-N(K''))$, matching meridian of K' to longitude of K'' and vice versa. L is the union of the components of L' and L'' other than K' and K''.

A *graph link* is a link obtained by splicing together *Seifert links*, that is links whose exteriors admit a Seifert fibration. The general Seifert link has the form $(\Sigma(\alpha_1, \ldots, \alpha_n), K_1 \cup \ldots \cup K_k)$ where $1 \leqq k \leqq n$ and $\alpha_1, \ldots, \alpha_n$ are pairwise coprime integers; it can be described as follows. If the α_i are all positive then $\Sigma(\alpha_1, \ldots, \alpha_n)$ is the unique 3-dimensional Seifert fibered homology sphere having fibers $K_1, \ldots, K_n$ of degrees $\alpha_1, \ldots, \alpha_n$ and no other exceptional fibers (fibers of degree >1). In particular, it only depends on the α_i's which are >1; it is the standard sphere if and only if at most two α_i's are not 1. It is oriented so that the linking number of any two fibers is positive (two general fibers then have linking number $\alpha_1 \ldots \alpha_n$). $(\Sigma(0, 1, \ldots, 1), K_1 \cup \ldots \cup K_n)$ is the link consist-

[9] In general, by the same argument, the number of components at infinity of a reduced plane curve V is greater than or equal to the number of components of the associated multilink

ing of an unknot plus $(n-1)$ meridians of it in the standard sphere S^3. Finally, if some α_i's are negative then $(\Sigma(\alpha_1, \ldots, \alpha_n), K_1 \cup \ldots \cup K_k)$ is $(\Sigma(|\alpha_1|, \ldots, |\alpha_n|), K_1 \cup \ldots \cup K_k)$ with some orientations changed: reversing the sign of an α_i corresponds to simultaniously reversing the ambient orientation and the orientation of the component K_i.

We symbolize the link $(\Sigma(\alpha_1, \ldots, \alpha_n), K_1 \cup \ldots \cup K_k)$ by the *splice diagram*

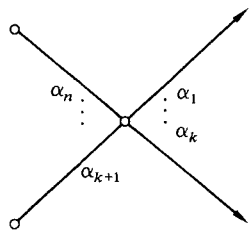

In particular, the link $\mathscr{H}_n = (S^3, K_1 \cup \ldots \cup K_n)$ consisting of n fibers of the Hopf fibration is symbolized by the splice diagram

(if $n=1$ or 2 the diagram may be abbreviated to $\circ\!\!\rightarrow$ or $\longleftrightarrow$ respectively).

A diagram such as

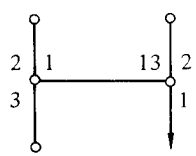

symbolizes the result of splicing the two Seifert links represented by the splice diagrams

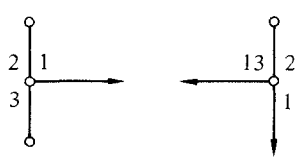

in the obvious way (this example represents the (2, 13)-cable on a (2, 3) torus knot or "trefoil"). More generally, splicing together any number of Seifert links

can be symbolized by analogously "splicing together" the corresponding splice diagrams. Thus any graph link (Σ, L) can be represented by a splice diagram Γ.

As a special case of splicing, each of the diagrams

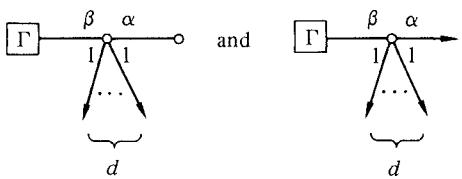

represents the result of doing an (α, β) cabling operation to the link represented by the splice diagram $\boxed{\Gamma}\!\!\rightarrow$. The precise operation is respectively replacing a component K by, or adding, d parallel (α, β) cables on K.

By attaching integer weights to the arrowhead vertices of a splice diagram to represent multiplicities, one can symbolize a graph multilink. This splice diagram is not unique:

(i) One can change the signs of an even number of weights around any vertex if one simultaniously changes the signs of the multiplicity weights at all arrowheads separated from that vertex by the edges corresponding to the changed weights.

(ii) An edge of the form

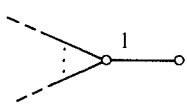

is redundant in a splice diagram and may be omitted (with its right hand vertex).

(iii) A vertex of valency 2 (that is, with just 2 adjoining edges) may be deleted, replacing the two adjoining edges by a single one.

(iv) An edge of the form

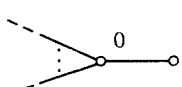

corresponds to a splitting of the link along embedded 2-spheres in Σ; we can delete this edge and all directly neighboring edges to represent the link by a disconnected splice diagram.

(v) Finally, any edge with zero "determinant" (see below) can be collapsed, coalescing the vertices at its two ends to one vertex (the signs of multiplicity weights at some arrowheads may also need to be changed).

Using these moves, any splice diagram for a graph link can be reduced to a *minimal* splice diagram (i.e. least number of vertices), and this minimal diagram is unique up to the allowable changes of signs of its weights. The minimal diagram is connected if and only if the graph link is irreducible.

We classify three types of vertex in a splice diagram Γ: *arrowheads* (corresponding to link components), *leaves* (non-arrowhead vertices of valency 1) and *nodes* (vertices of valency >1). For an edge E connecting two nodes of Γ as follows,

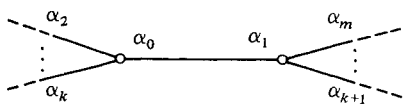

we define the *determinant* of the edge to be $d(E)=\alpha_0\alpha_1-\alpha_2\ldots\alpha_m$. Corresponding to the edge there is a torus in the ambient sphere Σ along which two Seifert splice components were pasted; $d(E)$ is the intersection number in this torus of typical fibers of the Seifert fibrations on each side of it. In particular, if $d(E)=0$ then the Seifert fibered structures can be isotoped to match up along this torus, so the splice decomposition was not minimal.

The following proposition will be used later.

Proposition 3.1 [E-N, Sect. 9]. *A link $\mathscr{L}=(S^3, L)$ is the link of some complex plane curve singularity if and only if it has a connected splice diagram with all weights and all edge determinants positive. It then has a minimal splice diagram with these properties.* □

For each node of a splice diagram we pick a typical fiber of the Seifert fibered structure of the corresponding Seifert link splice component and for each leaf we choose the corresponding exceptional fiber; we call these curves virtual components for the link; this agrees with the definition in the Introduction.

Lemma 3.2 [E-N, Sect. 10]. *The linking number in Σ of any two components (virtual or genuine) for the link is the product of all weights adjacent to, but not on, the simple path in the splice diagram connecting the corresponding vertices.* □

For example, for the (2, 13) cable on the trefoil whose splice diagram was pictured above, the knot itself has linking number $2.3.2=12$ with a typical fiber of the trefoil splice component.

An easy induction on the number of nodes in a splice diagram proves the following lemma.

Lemma 3.3. *The weights in a splice diagram are determined by all linking numbers of pairs of components (virtual or genuine) for the represented link.* □

We are now prepared to describe the effect of Dehn surgery on graph links. Let

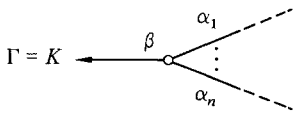

be a splice diagram for a link $\mathscr{L}=(\Sigma, L)$, where K is some component of L. If we perform $(1/k)$-Dehn surgery on the component K then Σ is replaced by a new homology sphere Σ' and the core of the Dehn surgery together with the remaining components of L thus give us a new link $\mathscr{L}'=(\Sigma', L')$. We wish to describe a splice diagram Γ' for $\mathscr{L}'$.

We shall call weights on edges of Γ far or near according as they are on the far or near end of an edge as viewed from the K vertex. We construct a splice diagram

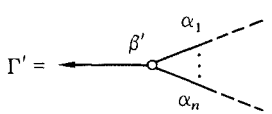

as follows. Γ' has the same shape as Γ; all near weights are unchanged from Γ; the far weights are determined inductively by:

(i) $\beta'=\beta-k\alpha_1\ldots\alpha_n$,

(ii) all edge determinants in Γ' are unchanged from Γ.

Equivalently (as an easy computation shows)

(iii) the far weight β_v at each node v is replaced by $\beta_v-k\lambda_v^2\alpha_v$, where α_v is the product of the near weights at the vertex v and λ_v is the product of all weights adjacent to but not on the simple path from v to the K arrowhead, excluding the near weights at v. (Thus $\lambda_v\alpha_v$ is the linking number with K of the virtual component corresponding to v.)

Proposition 3.4. *The above splice diagram Γ' is a splice diagram for $\mathscr{L}'$.*

Proof. The same tori that divide the exterior of the link $\mathscr{L}$ into Seifert fibered pieces also divide the exterior of $\mathscr{L}'$ into Seifert fibered pieces, giving a splice decomposition for $\mathscr{L}'$. Thus the shape of Γ' is correct. To see that the weights are correct it is sufficient, by Lemma 3.3, to see that they give correct linking numbers between components (both real and virtual) of $\mathscr{L}'$. But $(1/k)$ Dehn surgery on K replaces the linking number $\text{link}(S_1, S_2)$ of any two curves disjoint from K by $\text{link}(S_1, S_2)-k.\text{link}(S_1, K).\text{link}(S_2, K)$ while the linking number with

K of a curve disjoint from K is unchanged. Using (iii) it is easy to see that the described change of weights to get Γ' from Γ has the correct effect on linking numbers. □

Example. $(1/k)$ Dehn surgery on an (p, q) torus knot in S^3 gives a knot in the homology sphere $\Sigma(p, q, 1-kpq)$. The splice diagrams are:

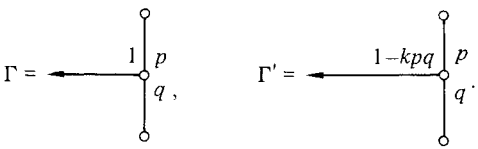

4. Proof of Theorem 2: RPI diagrams for links at infinity

Recall that a *rooted splice diagram* is one with a chosen *root vertex*:

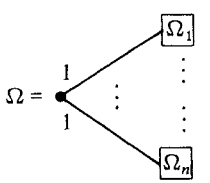

(the root vertex is marked "•"). (4.1)

All weights at the root vertex equal 1. The diagram may be non-minimal as a splice diagram—it certainly is if $n=2$. If $n=1$, the weight 1 at the root vertex should be disregarded when considering Ω as a splice diagram. The end of any edge which is furthest from the root vertex is called the *far end* and the other end the *near end* of the edge. Weights on edges are also correspondingly called *near* or *far*. Recall that Ω is an *RPI splice diagram* if

(0) at most one near weight at each vertex is not equal to 1;

(i) all near weights are positive;

(ii) all edge determinants are negative (we include the edges at the root vertex in this condition, even when $n=1$).

The first part of Theorem 2 associates a specific RPI splice diagram Ω to a reduced plane curve $V \subset \mathbb{C}^2$ plus an embedding $\mathbb{C}^2 \subset \mathbb{P}^2$. We must thus study the link at infinity of $V = C - (C \cap \mathbb{P}^1) \subset \mathbb{P}^2 - \mathbb{P}^1 = \mathbb{C}^2$, where C is a reduced projective curve. We can assume that $\mathbb{P}^1$ is not a component of C, so C meets $\mathbb{P}^1$ in finitely many points $Y_1, \ldots, Y_n$, say. Choose an embedded disk D_0 in $\mathbb{P}^1$ which contains $C \cap \mathbb{P}^1$ and let D be a thin 4-disk regular neighborhood of D_0 in $\mathbb{P}^2$ whose boundary $S = \partial D$ meets C and $\mathbb{P}^1$ transversely (see Fig.).

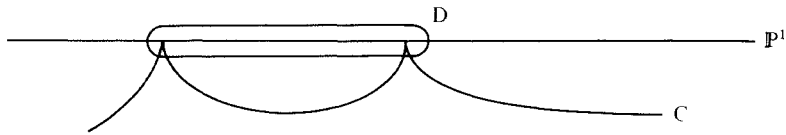

Then $(S, (\mathbb{P}^1 \cup C) \cap S)$ is a link $\mathscr{L}_0$ which can be represented by a splice diagram Γ (non-minimal if $n=1$) as follows:

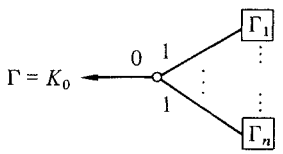

(4.2)

Here K_0 is the component $\mathbb{P}^1 \cap S$ and each $\leftarrow\boxed{\Gamma_i}$ is a splice diagram which represents the link of $\mathbb{P}^1 \cup C$ at the point Y_i. Since this latter is a singularity link, $\leftarrow\boxed{\Gamma_i}$ may be assumed to be a minimal splice diagram with all weights and all edge determinants positive (Proposition 3.1). The link represented by $\leftarrow\boxed{\Gamma_i}$ is a toral link (i.e. obtained by iterated cabling operations) and K_0 is unknotted. This is equivalent to saying that at most one near weight at each vertex is not equal to 1, where "near" is interpreted with reference to the K_0 vertex.

Now let $N\mathbb{P}^1$ denote a thin closed tubular neighborhood of $\mathbb{P}^1$ in $\mathbb{P}^2$, so $S^3 = \partial N\mathbb{P}^2$ is a "sphere at infinity" in $\mathbb{C}^2$, and $\mathscr{L}_1 = (S^3, S^3 \cap C)$ is the link at infinity that we are interested in. Note that $N\mathbb{P}^1$ is obtained from D by adding a 2-handle along $K_0 \subset S = \partial D$, so $\mathscr{L}_1$ is obtained from $\mathscr{L}_0$ by $(+1)$ Dehn surgery on K_0. Thus, by Proposition 3.4, $\mathscr{L}_1$ has a (non-minimal) splice diagram

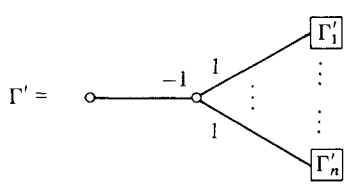

where the Γ_i' differ from the Γ_i only in that all far weights have been changed so as to keep all edge determinants the same as in Γ. Actually, this is still not quite the link we are interested in, since it is being viewed from "inside" $\mathbb{C}^2$, i.e. with the wrong ambient orientation. Reversal of ambient orientation is effected by reversing the signs of all far weights (which reverses the signs of all edge determinants). This gives a splice diagram of the form:

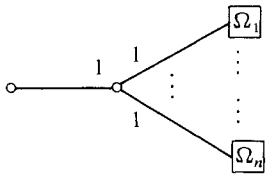

This is non-minimal and can be simplified to the (possibly still non-minimal) splice diagram

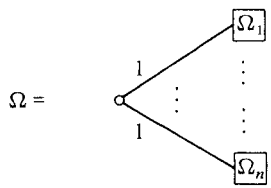

With the leftmost vertex as "root vertex," this has near weights still positive and all edge determinants negative, so it is an RPI splice diagram.

That $n_\infty(V)$ is the valency n of the root node is immediate from the construction. The degree $\deg(V)$ equals the intersection number of V and a generic line in $\mathbb{C}^2$. We can compute this intersection number in any sufficiently large disk $D^4 \subset \mathbb{C}^2$. But the intersection number of two relative 2-cycles in a disk D^4 is the linking number of their boundaries in ∂D^4. Moreover, the link at infinity of a generic line is a representative for the virtual component S_{root} for the root vertex. Thus $\deg(V) = l_{\text{root}}$, the linking number of S_{root} with L.

The above proof applies without change to show that a sublink of a link at infinity has an RPI splice diagram (in fact, it is easy to see that a sublink of a link with an RPI splice diagram has an RPI splice diagram). We now show, conversely, that a link which has an RPI splice diagram is a sublink of some link at infinity. The above procedure to derive Ω from Γ can be reversed to reconstruct Γ from the RPI diagram Ω. We first consider the case of a link given by an RPI splice diagram

$$\Omega = \bullet\!\!-\boxed{\Omega_1},$$

as in (4.1) above with $n=1$. Its corresponding diagram

$$\Gamma = \overset{0}{\leftarrow\!\!\circ}\!\!-^{1}\boxed{\Gamma_1}$$

has positive near weights and positive determinants. By induction, starting at the left of the diagram, one deduces that the far weights of $\leftarrow\boxed{\Gamma_1}$ are positive. Thus $\leftarrow\boxed{\Gamma_1}$ is a splice diagram for a singularity link, and it can be realized as the link at a point $Y_1 \in \mathbb{P}^1 \subset \mathbb{P}^2$ of a curve of the form $C_1 \cup \mathbb{P}^1$. Now, given the more general diagrams Ω and Γ as in (4.1) and (4.2) above, we realize each $\leftarrow\boxed{\Gamma_i}$ by the link of a curve of the form $C_i \cup \mathbb{P}^1$ at a point $Y_i \in \mathbb{P}^1$, making sure that the points Y_i are distinct. Then, putting $C = C_1 \cup \ldots \cup C_n$, the link

represented by Ω is a sublink of the link at infinity of $V = C \cap (\mathbb{P}^2 - \mathbb{P}^1) \subset \mathbb{P}^2 - \mathbb{P}^1 = \mathbb{C}^2$.

We must still show that our link is a sublink of some *good* link at infinity. Let $f(x, y) = 0$ be the defining polynomial for V. By applying an automorphism of the form $(x, y) \mapsto (x, y + x^N)$ for some large N, we can replace V by a V with just one point at infinity: $C = \bar{V}$ intersects $\mathbb{P}^1$ only in the point $x = z = 0$ in homogeneous coordinates (x, y, z) on $\mathbb{P}^2 = \mathbb{C}^2 \cup \mathbb{P}^1$. Let $h(x, y, z) = 0$ be the homogenized equation for C, of degree d say. In affine coordinates near $x = z = 0$, C is given by $h(x, 1, z) = 0$. Adding sufficiently high order terms $\alpha_i x^{p_i} z^{q_i}$ to this does not alter the link at this point, since an isolated singularity is finitely determined. $h(x, y, z)$ is replaced by

$$h_{\text{new}}(x, y, z) = y^{m-d} h(x, y, z) + \sum a_i x^{p_i} y^{m - p_i - q_i} z^{q_i}$$

with $m = \max\{p_i + q_i\}$, and $f(x, y)$ is replaced by $f_{\text{new}}(x, y) = h_{\text{new}}(x, y, 1)$. This adds new points at infinity, but it is easy to see that, after a generic such replacement, the additional intersection points of the new curve C_{new} with $\mathbb{P}^1$ are all distinct and transverse. Any other fiber of $f_{\text{new}}(x, y)$ has homogeneous equation $h_{\text{new}}(x, y, z) + cz^m = 0$. Away from $x = 0$ this intersects $\mathbb{P}^1$ transversely in the same points as C_{new}. If m is large then, by finite determination, it has an equivalent singularity to $h_{\text{new}}(x, y, z) = 0$ at $x = z = 0$. It follows that f_{new} is good.

To complete the proof of Theorem 2 we must show that if $\mathscr{L}$ is the whole link at infinity of a regular plane curve $V = C - (C \cap \mathbb{P}^1) \subset \mathbb{P}^2 - \mathbb{P}^1 = \mathbb{C}^2$ then the resulting diagram Ω is regular. We use the notation of the beginning of this section: C meets $\mathbb{P}^1$ in points $Y_1, \ldots, Y_n$; Γ is the corresponding splice diagram as in (4.2) and Ω is the resulting RPI splice diagram for $\mathscr{L}$ as in (4.1). For each i let $\mathscr{L}_i = (S^3, L_i)$ denote the link with splice diagram $\circ\!\!-\!\!\boxed{\Gamma_i}$; that is, the local link of the curve C at the point Y_i (we call this a "singularity link" whether or not C happens to be singular at Y_i). Let K_i be the virtual component represented by the leftmost vertex. A nonsingular deformation $\bar{C}$ of C will be isotopic to $F_0 \cup F_1 \cup \ldots \cup F_n$, where F_0 is a Seifert surface for $\mathscr{L}$ (isotopic to F) and F_i is a fiber of the singularity link $\mathscr{L}_i$ (see Fig.).

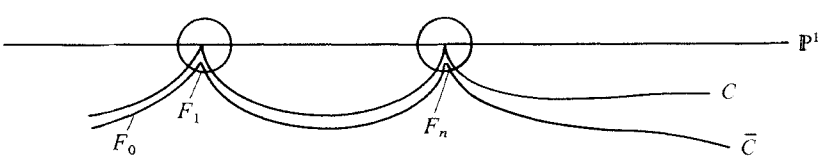

In particular, it has euler characteristic $\chi(\bar{C}) = \sum_{i=0}^{n} \chi(F_i)$. Now let P_i denote the local intersection number of C with $\mathbb{P}^1$ at Y_i, so the total intersection number

of C with $\mathbb{P}^1$ is $P=\sum_{i=1}^{n} P_i$. Then $\bar{C}$ has degree P, so its euler characteristic is $\chi(\bar{C})=3P-P^2$. Thus

$$3P-P^2=\sum_{i=0}^{n}\chi(F_i). \tag{4.3}$$

Note that P_i can also be interpreted as the linking number $\mathrm{link}(K_i, L_i)$ for the link $\mathscr{L}_i$, and $P=\mathrm{link}(K_0, L_0)$, computed for the link L_0.

We need to introduce some notation to continue the calculation. The far weight at a vertex v in Γ will be denoted β_v, so the far weight at v in Ω is $\beta_v''=\lambda_v^2\alpha_v-\beta_v$ in the notation of Proposition 3.4. For two vertices v and w in a splice diagram, we denote by $v\cdot w$ the vertex closest to the root vertex on the simple path from v to w and by $\alpha(v, w)$ the product of all near weights adjacent to but not on this path. Thus $\alpha(v, w)\beta_{v\cdot w}$ is the linking number of the components (virtual or genuine) corresponding to v and w. Finally, $\Gamma^{\rightarrow}$ and Γ° will denote the set of arrowheads resp. non-arrowheads in any splice diagram Γ, and the valency (number of incident edges) for any $v\in\Gamma^{\circ}$ will be denoted δ_v.

For each node or leaf v of Ω, recall that S_v denotes the corresponding virtual component and $l_v=\mathrm{link}(S_v, L)$. By Proposition 3.2, if v is in Ω_i,

$$l_v=\lambda_v\alpha_v(P-P_i)+\sum_{w\in\Gamma_i^{\rightarrow}}\alpha(v, w)\beta''_{v\cdot w}. \tag{4.4}$$

Since F_0 is a minimal Seifert surface for $\mathscr{L}$, [E-N, Theorem 11.1] says

$$\chi(F_0)=(2-n)P+\sum_{i=1}^{n}\sum_{v\in\Gamma_i^{\circ}}(2-\delta_v)\,|l_v|. \tag{4.5}$$

Let χ_0 denote the result of removing the absolute value signs in (4.5). Then it is not hard to see that $\chi_0\geqq\chi(F_0)$, with equality if and only if each l_v is non-negative (a leaf v contributes the wrong way when removing the absolute values, but its contribution is overwhelmed by the contribution of the adjacent node). Thus to complete the proof of Theorem 2 we must show $\chi_0=\chi(F_0)$. To do so we will verify that (4.3) is valid with $\chi(F_0)$ replaced by χ_0.

By [E-N, Theorem 11.1] again,

$$\chi(F_i)=P_i+\sum_{v\in\Gamma_i}(2-\delta_v)\sum_{w\in\Gamma_i^{\rightarrow}}\alpha(v, w)\beta_{v\cdot w}, \tag{4.6}$$

so, since $\beta''_{v\cdot w}+\beta_{v\cdot w}=\lambda^2_{v\cdot w}\alpha_{v\cdot w}$, adding the Eqs. (4.6) to (4.5) with absolute values removed and using (4.4) gives

$$\chi_0+\sum_{i=1}^{n}\chi(F_i)=(3-n)P$$
$$+\sum_{i=1}^{n}\sum_{v\in\Gamma_i^{\circ}}(2-\delta_v)\Big(\lambda_v\alpha_v(P-P_i)+\sum_{w\in\Gamma_i^{\rightarrow}}\alpha(v, w)\lambda^2_{v\cdot w}\alpha_{v\cdot w}\Big). \tag{4.7}$$

Let $\alpha(o, v)$ be the linking number of K_0 with the (virtual or genuine) component for v. Then $\lambda_v \alpha_v = \alpha(o, v)$ and $\alpha(v, w)\lambda_{v\cdot w}^2 \alpha_{v\cdot w} = \alpha(o, v)\,\alpha(o, w)$, so (4.7) simplifies to

$$\begin{aligned}
&\chi_0 + \sum_{i=1}^{n} \chi(F_i) \\
&\quad = (3-n)P + \sum_{i=1}^{n} \sum_{v \in \Gamma_i^\circ} (2-\delta_v)\,\alpha(o, v)((P-P_i) + \sum_{w \in \Gamma_i^{\rightarrow}} \alpha(o, w)) \\
&\quad = (3-n)P + \sum_{i=1}^{n} \sum_{v \in \Gamma_i^\circ} (2-\delta_v)\,\alpha(o, v)((P-P_i) + P_i) \\
&\quad = (3-n)P + P \sum_{i=1}^{n} \sum_{v \in \Gamma_i^\circ} (2-\delta_v)\,\alpha(o, v). \qquad (4.8)
\end{aligned}$$

On the other hand, let Γ_i^* and $\Gamma_i^\bullet$ be the nodes and leaves respectively of Γ_i and let E_v denote a set of $\delta_v - 2$ outgoing edges at v whose near weights are 1 (recall that at most one near weight at v is not 1; its value will be α_v). Then

$$\begin{aligned}
\sum_{v \in \Gamma_i^\circ} (2-\delta_v)\,\alpha(o, v) &= \sum_{v \in \Gamma_i^*} \sum_{e \in E_v} (-\alpha(o, v)) + \sum_{v \in \Gamma_i^\bullet} \alpha(o, v) \\
&= \sum_{v \in \Gamma_i^*} \sum_{e \in E_v} (-\alpha(o, v)) + \sum_{v \in \Gamma_i^\bullet \cup \Gamma_i^{\rightarrow}} \alpha(o, v) - P_i \\
&= 1 - P_i,
\end{aligned}$$

where the last equality is a simple induction on the size of the diagram. Substituting this into (4.8) gives

$$\begin{aligned}
\chi_0 + \sum_{i=1}^{n} \chi(F_i) &= (3-n)P + P \sum_{i=1}^{n} (1-P_i) \\
&= 3P - P^2,
\end{aligned}$$

as was to be proved. □

Remark 4.1. We do not really need to know that F, or equivalently F_0, is a minimal Seifert surface for the above proof. In fact the proof implies it, for without assuming it we just have inequalities $\chi(F_0) \leqq$ (right side of (4.5)) $\leqq \chi_0$ and the proof shows that both these inequalities are equalities.

Definition 4.2. For a reduced plane curve $V \subset \mathbb{C}^2$ plus an embedding $\mathbb{C}^2 \subset \mathbb{P}^2$, Theorem 2 gives a specific RPI diagram Ω which we call *the associated RPI splice diagram.* The corresponding diagram Γ as in (4.2) is a minimal splice diagram if $n_\infty > 1$ and it is minimal once the vertex next to the root has been suppressed if $n_\infty = 1$. We call this minimal version of Γ *the splice diagram at infinity for* Ω. Ω itself is not generally minimal (even as an RPI diagram), but Theorem 3 says that any minimal RPI diagram is the associated diagram for some embedding $\mathbb{C}^2 \subset \mathbb{P}^2$.

We close this section with a useful corollary of the above proof. Let $V \subset \mathbb{C}^2$ be a nonsingular plane curve, regular or not, and let $\mathscr{L}$ be its link at infinity. Let Ω be the RPI splice diagram for $\mathscr{L}$ associated to some embedding $\mathbb{C}^2 \subset \mathbb{P}^2$ (e.g. any minimal RPI diagram for $\mathscr{L}$). It is not hard to see that (4.3) is valid with $\chi(F_0)$ replaced by $\chi(V)$. On the other hand, the computation of the proof still applies to show that (4.3) is valid with $\chi(F_0)$ replaced by χ_0 defined as before (Eq. 4.5 with absolute values removed). Thus $\chi(V)=\chi_0$. Now if V is singular but still reduced, then this formula must be adjusted using the euler characteristics χ_p of the Milnor fibers of the singularities p of V. We thus get the following Theorem.

Theorem 4.3. *If $V \subset \mathbb{C}^2$ is a reduced plane curve and Ω is a minimal* RPI *splice diagram for its link $\mathscr{L}$ at infinity then*

$$\chi(V)=\sum_{v\in\Omega^\circ}(2-\delta_v)l_v+\sum_p \mu_p,$$

where the second sum is over the singularities p of V and $\mu_p=1-\chi_p$ is the Milnor number of the singularity at p. □

If V is nonsingular and l_v is replaced by $|l_v|$ this formula is just the formula of [E-N, Theorem 11.1] for the euler characteristic of a minimal Seifert surface of $\mathscr{L}$, so if $\mathscr{L}$ is an irregular toral link (some l_v is negative) then $\chi(V)$ definitely exceeds the euler characteristic of a minimal Seifert surface for $\mathscr{L}$. Conjecturally this is always the case if V is not a regular curve (see Sect. 9).

5. Basic properties of RPI diagrams and regular toral links

Let Ω be an RPI splice diagram for a link $\mathscr{L}'=(S^3, L)$ as in (4.1) above. Recall that for any node or leaf v we denote $l_v=\text{link}(S_v, L)$ where S_v is the corresponding virtual component, and Ω is called a *regular splice diagram* and $\mathscr{L}$ is called a *regular toral link* if these l_v are all non-negative.

If v is a leaf and w is the adjacent node, then $l_v=l_w/\alpha_w$ (notation α_w as in the previous section), so the non-negativity of the l_v for leaves follows from the non-negativity for nodes. The following proposition will be used often.

Proposition 5.1. *Let e be an edge of Ω connecting two nodes and denote the nodes at its near and far end by v and w respectively. Let α be the weight at the near end of e (so $\alpha=1$ or α_v). Then $\alpha_w l_v > \alpha l_w$.*

Corollary 5.2. *The condition for Ω to be a regular splice diagram—the l_v should be non-negative for all nodes and leaves v—need only be prescribed for the nodes v furthest from the root vertex; the l_v will then be positive for all other nodes.* □

Proof of Proposition. Let β be the product of the weights other than α at node v. Removing edge e splits Ω into two pieces; let L_v be the union of components of L corresponding to arrowheads in the piece containing node v and L_w the

union of components corresponding to arrowheads in the piece containing w. Then

$$l_v = \text{link}(S_v, L_v) + \text{link}(S_v, L_w) = \text{link}(S_v, L_v) + \frac{\beta}{\beta_w}\text{link}(S_w, L_w),$$

$$l_w = \text{link}(S_w, L_v) + \text{link}(S_w, L_w) = \frac{\alpha_w}{\alpha}\text{link}(S_v, L_v) + \text{link}(S_w, L_w),$$

where the second equality in each case is by Lemma 3.2. These two equations imply

$$\alpha_w l_v - \alpha l_w = \frac{-d(e)}{\beta_w}\text{link}(S_w, L_w),$$

where $d(e) = \alpha\beta_w - \beta\alpha_w$ is the determinant of the edge e. But $\frac{1}{\beta_w}\text{link}(S_w, L_w)$ is positive, since its computation by Lemma 3.2 only involves near weights, and $-d(e)$ is positive by the reverse Puiseux inequalities. □

Corollary 5.3. *A regular toral link is the boundary of a fiber of a unique multilink with no zero multiplicities, and any minimal Seifert surface for it is isotopic to a fiber of the multilink.*

Proof. Once we have found the multilink, its uniqueness and the statement about minimal Seifert surfaces is by Theorem 5. Let v be a node with $l_v = 0$. We must show that this node has the form

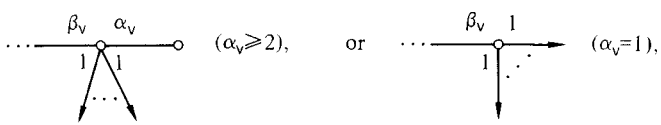

with k_v arrowheads, say. For replacing each such node by an arrowhead with multiplicity $k_v\alpha_v$ then gives the desired multilink. But by Corollary 5.2, the only other possible form for v is

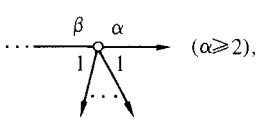

and by Lemma 3.2 this would imply $l_v \equiv \beta (\text{mod}\,\alpha)$, in contradiction to the assumption that $l_v = 0$. □

We have also shown:

Proposition 5.4. *The multilink associated to a regular toral link has a splice diagram satisfying the reverse Pulseux inequalities, with all multiplicities positive, and with the l_v positive for all nodes v.* □

We close this section with a useful observation about RPI splice diagrams. It is immediate from the RPI condition.

Lemma 5.5. *If a far weight in an* RPI *diagram is negative, then so are all far weights which are beyond it from the point of view of the root node.* □

6. Minimal RPI splice diagrams

The basic result of this section is that for a link of interest to us, "minimal" RPI diagrams can differ only in the position of the root vertex. We first discuss the case of regular toral links and then describe the situation for links at infinity which are not necessarily regular.

It is convenient to exclude the following small "exceptional" splice diagrams from the general discussion (in each case the root note is designated by a "●" symbol):

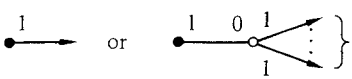

(6.1)

Each of these diagrams represents a link consisting of $d \geqq 1$ unlinked unknotted circles: – the link at infinity $\mathscr{L}(x^d - 1, \infty)$.

Now let $\mathscr{L}$ be a regular toral link and let

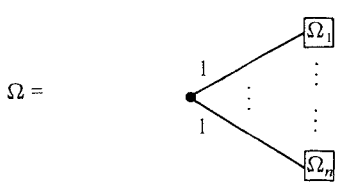

(6.2)

be a regular splice diagram for $\mathscr{L}$ not as in (6.1). If $n=1$ then the far edge weight closest to the root vertex must be >0 (it cannot be negative because of regularity and if it were zero then, by Proposition 5.1, Ω would be an excluded diagram (6.1)).

Definition. We will call a regular splice diagram Ω a *minimal RPI diagram* if it is one of the diagrams (6.1), or if it is as in (6.2) and each $\leftarrow\boxed{\Omega_i}$ is minimal and, if $n=1$, the far edge weight closest to the root vertex is >1. That is, Ω is not of the form:

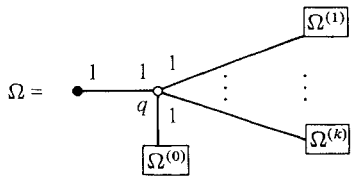

(6.3)

If Ω does have this form then we shall see later that there is a smaller RPI diagram for the same link.

If we forget which vertex of a minimal regular RPI diagram Ω is root vertex then we get a minimal splice diagram except if $n=2$, in which case we can suppress the root vertex, coalescing the two adjoining edges to one. Either way, we denote the resulting splice diagram by Ω_0.

Lemma 6.1. *If Ω is not one of the following diagrams* (6.4) *or* (6.4)′ *then Ω_0 is a minimal splice diagram.*

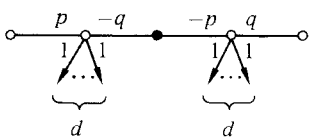

$(p>q>1,\ d\geqslant 1)$ (6.4)

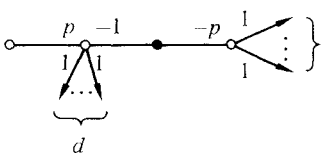

$(p>1,\ d>1).$ (6.4)′

(The diagram (6.4)′ is a reduced version of (6.4) in the case $q=1$ and $d>1$. A minimal splice diagram for the link represented by (6.4) or (6.4)′ is as follows; omitted edge weights are 1:

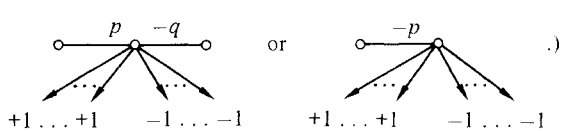

.)

Proof of Lemma. If Ω_0 is not minimal then it has an edge which connects two nodes and has edge determinant 0. This edge arose by suppressing a root vertex of valency 2 in Ω. Since Ω has negative edge determinants, it is easy to see that both weights on this edge must be negative. Let v and w be the nodes at its ends. Lemma 3.2 implies that the linking numbers l_v and l_w (notation as in Sect. 5) are the negatives of each other. Since they are non-negative by assumption, they are both 0. Corollaries 5.2 and 5.3 now imply that Ω must be one of the diagrams (6.4) or (6.4)′. □

Ω can be recovered from Ω_0 by choosing an existing vertex as root vertex or introducing a root vertex on some edge. We shall call any splice diagram Ω_0 for our link $\mathscr{L}$ *rootable* if it can be *rooted*: turned into a regular splice diagram in this way.

We wish to bound the number of ways of rooting Ω_0. To do this, we construct a subtree of Ω_0 which contains all the possible places for introducing a root vertex. Namely, we first delete any edge of Ω_0 which satisfies one of the following two conditions:

– there is a non-positive weight adjacent to (but not on) the given edge;

– there are two weights unequal to 1 adjacent to the given edge at one end of it.

Then there is one component of what is left, we call it root(Ω_0), which contains all the possible places for a root vertex. Indeed, any potential root vertex outside this component would either have a negative near weight or would correspond to a knotted virtual link component. Each node of root(Ω_0) is either of valency 2 with both weights greater than 1 or of valency >2 with all weights positive and at most one weight greater than 1. If exactly one weight is greater than 1, we call the node a *contributing node*. For such a node v let δ_v denote its valency in Ω_0.

Theorem 6.2. *Let $\mathscr{L}$ be a regular toral link. Then either $\mathscr{L}$ is given by one of the diagrams* (6.1), (6.4), *or* (6.4)′, *and this diagram is the unique minimal* RPI *diagram for $\mathscr{L}$, or $\mathscr{L}$ has a unique rootable minimal splice diagram Ω_0 and every minimal* RPI *splice diagram for $\mathscr{L}$ results from rooting Ω_0. The number of ways of doing this is $1+\sum(\delta_v-2)$, sum over all contributing nodes of* root(Ω_0).

Example. The following is a picture of a typical root (Ω_0). The dotted lines indicate edges not in root(Ω_0) and possible positions for a root vertex are marked by a "●" symbol. There are just two contributing nodes, each of valency 3.

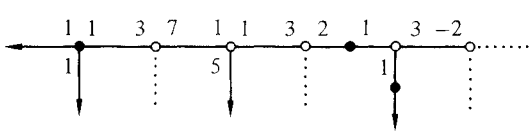

Lemma 6.3. *If $\mathscr{L}$ is a regular toral link then $\mathscr{L}$ has at most one minimal splice diagram Ω_0 which is rootable.*

Proof. First some terminology. If root(Ω_0) consists of a single edge then we call this edge the *root edge*. An edge with non-negative determinant or an edge with an arrowhead at one end and a non-positive weight at the other must be a root edge.

We must show that if Ω_0 is a rootable minimal splice diagram for $\mathscr{L}$ then it is no longer rootable if the signs of its weights are changed in any admissible way (i.e. without changing the represented link). Note that a rootable diagram has at most one non-positive weight at each vertex. Suppose there is an admissible change of signs of weights of Ω_0 which results in a rootable diagram Ω_0'.

Since an admissible change of weights changes an even number of weights at any vertex, a vertex affected by the change has just one negative weight both before and after the change, and just these two weights are changed. Call the corresponding two edges at this vertex "changed edges." This change switches the signs of the edge determinants of these two edges. Since at most one edge determinant in each of Ω_0 and Ω'_0 is non-negative, it follows that the set of changed edges in Ω_0 must form a path from a leaf to a leaf, or from a leaf to a root edge of Ω_0 or Ω'_0, or from root edge of Ω_0 to root edge of Ω'_0. In the first two cases, at least one of Ω_0 and Ω'_0 has a negative weight on an edge ending in a leaf, which is impossible, since the root vertex would have to be this leaf, and the weight closest to it cannot be negative. In the third case the situation is as follows (the p_i and q_i are positive, unmarked edge weights are 1, each of v_1 and v_s may be an arrowhead instead of a node, and the RPI condition implies that at most one of v_2 through v_{s-1} is of the "exceptional" type indicated in the middle):

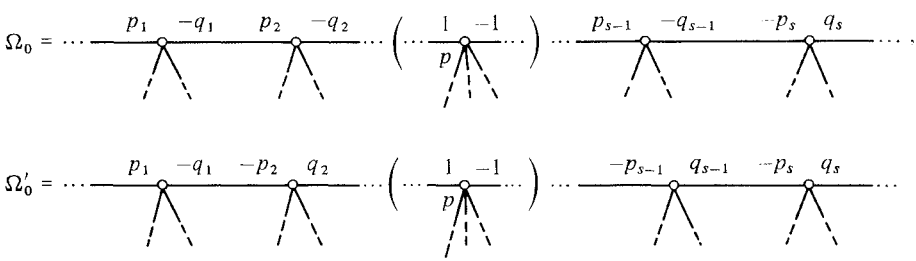

If there are arrowheads "below" nodes v_2 through v_{s-1} then the corresponding link components of $\mathscr{L}$ have the wrong orientation after the change (one can change the orientation of *all* components without changing the link: – toral links are invertible – but changing the orientation of only some of them does change the link, since it changes linking numbers). Thus there are no such arrowheads, so $s=3$ and v_2 is of the exceptional type. The non-negativity of l_{v_2} in both Ω_0 and Ω'_0 now shows $l_{v_2}=0$, contradicting Corollary 5.2 (except in the case that v_1 and v_3 are both arrowheads, in which case Ω_0 is isomorphic to Ω'_0). □

Proof of Theorem 6.2. We first show that a minimal RPI diagram exists by induction on the size. Suppose therefore that $\mathscr{L}$ is given by an RPI diagram as in (6.2) which is non-minimal. If an $\leftarrow\boxed{\Omega_i}$ is non-minimal we can reduce it, keeping the RPI property, thus reducing the size of Ω. Thus we can assume Ω is as in (6.3). If $k=1$ then we get a smaller RPI diagram for $\mathscr{L}$ replacing q by 1 and collapsing the edge at the root vertex and then also deleting the portion $—\boxed{\Omega^{(0)}}$ if it has the form —○. If $k>1$ then we obtain a splice diagram Ω_0 for $\mathscr{L}$ by deleting the root vertex and its adjacent edge; the following computation then shows that this Ω_0 is rootable to get an RPI diagram (in at least k different ways).

It remains to count the number of ways of rooting a given Ω_0. We bisect each edge of root(Ω_0) and direct each resulting half-edge as follows:
- at a node with all weights 1, direct the half-edges away from the node;
- at a node with one weight larger than the others, direct the half-edge with larger weight away from the node and the others toward the node;
- at a leaf or arrowhead of the subtree direct the half-edge outward.

This gives a flow on root(Ω_0) and the possible positions for a root vertex are precisely the sources of this flow. The desired formula is now an easy induction on the number of contributing vertices. □

Remark. Non-equivalent regular toral links which are equivalent as unoriented links would have to be related as in the proof of 6.3. Let Ω and Ω' be the RPI diagrams resulting from that proof. An easy calculation shows that l_{v_2} cannot be non-negative for both Ω and Ω'. Thus:

Proposition 6.4. *Non-equivalent regular toral links can never be equivalent as unoriented links.* □

Irregular plane curves

For a link at infinity of a reduced but not necessarily regular algebraic curve V one has similar results. Let Ω be its RPI splice diagram as in (6.2) above, constructed as in Sect. 4. First note that if $n=1$ then the far weight closest to the root vertex cannot be negative, and is zero only if Ω is as in (6.1) and V is a union of parallel lines. (This follows by observing that if the weight is non-positive then, in the notation of Sect. 4, the curve $C=\bar{V}$ is transverse to $\mathbb{P}^1$ at its point at infinity, and since it meets $\mathbb{P}^1$ nowhere else, its multiplicity at that point must equal its degree, making it a union of lines through that point.) We can thus define Ω to be *minimal* as an RPI diagram as before.

Theorem 6.5. *The analog of Theorem* (6.2) *still holds: If Ω_0 is not minimal then there is just one minimal* RPI *splice diagram and if Ω_0 is minimal, then it is the unique rootable minimal splice diagram for $\mathscr{L}$ and the count of the number of ways of rooting it still applies.*

Proof. The main difference is the analysis of the case that Ω_0 has an edge with determinant 0 – there are more cases than in Lemma 6.1 and one must show that there is still just one minimal RPI splice diagram for the link in such a case. As before, the weights on the determinant 0 edge must be negative, so by Lemma 5.5 every far weight is negative. Let Ω_1 be the result of collapsing this edge of Ω_0 (suitable arrowheads of Ω_1 must be given an orientation weight -1 to represent the correct orientations of link components of $\mathscr{L}$). Call the node that results from this collapse the root node. Ω_1 is a minimal splice diagram with exactly one negative weight at each node. To recover Ω_0 from Ω_1, we must be able to recognize the root node and also recognize how to partition the edges at that node into two sets corresponding to the two vertices that collapsed into it; moreover, we must even be able to do this after admissible sign changes in Ω_1. The linking number of two components of $\mathscr{L}$ is positive

if and only if the path in Ω_0 connecting the corresponding arrowheads passes through the root edge. Once the root node is known, this determines the partition of edges at it. But it also severely restricts the positions for the root node in Ω_1, and the RPI condition now easily pinpoints it precisely.

We must also show that the analog of Lemma 6.3 still holds. The proof only used that Ω is an RPI diagram, except for its appeal to the non-negativity of l_{v_2} for the final case. This case cannot occur for a link at infinity: by Proposition 8.6, if the root node of Ω has valency 2 then the resulting edge of Ω_0 has non-positive edge determinant; thus Ω and Ω' cannot both be RPI diagrams (except in the harmless case that v_1 and v_3 are both arrowheads). □

7. Proof of Theorem 3: minimal RPI diagrams for links at infinity

Let $V \subset \mathbb{C}^2$ be a reduced algebraic curve and $\mathscr{L}$ its link at infinity. We first show that there is a minimal embedding of $\mathbb{C}^2$ in $\mathbb{P}^2$ for V, that is, one whose associated RPI for diagram for $\mathscr{L}$, as constructed as in Sect. 4, is minimal.

Choose any embedding of $\mathbb{C}^2$ in $\mathbb{P}^2$, so $\mathbb{C}^2 = \mathbb{P}^2 - \mathbb{P}^1$. Let Ω be the associated RPI splice diagram for the link $\mathscr{L}$ and suppose that Ω is not a minimal RPI diagram. Then, by definition, Ω must have the form

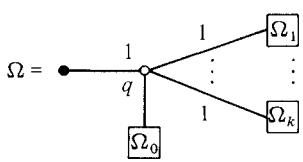

with $q > 1$. (7.1)

Lemma 7.1. *After a linear change of coordinates, the defining polynomial $f(x, y)$ for V has the form*

$$f(x, y) = x^s \prod_{\nu=1}^{k} (x^q - \alpha_\nu y)^{r_\nu} + \sum_{\substack{i,j \geq 0 \\ qj+i<qr+s}} c_{ij} x^i y^j, \tag{7.2}$$

where $r = \sum r_\nu$ and the r_ν are positive integers and the α_ν are distinct nonzero constants.

Given this lemma, the existence of a minimal embedding $\mathbb{C}^2 \subset \mathbb{P}^2$ for V follows by induction on degree, since if $f(x, y)$ is in the form (7.2), then the transformation $(x, y) \mapsto \left(x, y + \frac{1}{\alpha_1} x^q\right)$ takes $f(x, y)$ to a polynomial of strictly lower degree.

Proof of lemma. By a linear change of coordinates we may assume that the point at infinity of V occurs at $x=0$. Then, after multiplying by a constant if necessary, the defining polynomial $f(x, y)$ has the form

$$f(x, y)=x^d+(\text{lower order}).$$

Let the homogenization of $f(x, y)$ be $h(x, y, z)$. Then the equation for $C=\bar{V}$ in affine coordinates (x, z) about the point at infinity is $g(x, z)=0$, where $g(x, z)=h(x, 1, z)$. $g(x, z)$ has the form

$$g(x, y)=x^d+z\,g_0(x, z),$$

where $g_0(x, z)$ has degree $\leqq d-1$.

The associated splice diagram at infinity for Ω is

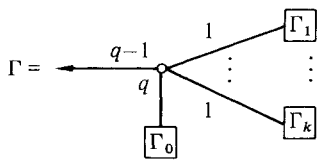

That is, this is the splice diagram for the link of the singularity at $x=z=0$ of $z\,g(x, z)=0$, with the leftmost arrowhead corresponding to the branch $\mathbb{P}^1=(z=0)$. The link of the singularity of $g(x, z)=0$ at $(0, 0)$ has splice diagram

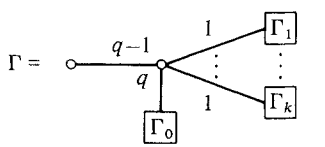

We now consider the Newton polygon for $g(x, z)$, that is, the convex hull of the set of points $(a, b)\in\mathbb{R}^2$ for which $x^a z^b$ occurs as a monomial in $g(x, z)$, together with the points $(\infty, 0)$ and $(0, \infty)$. We claim that its boundary has the form:

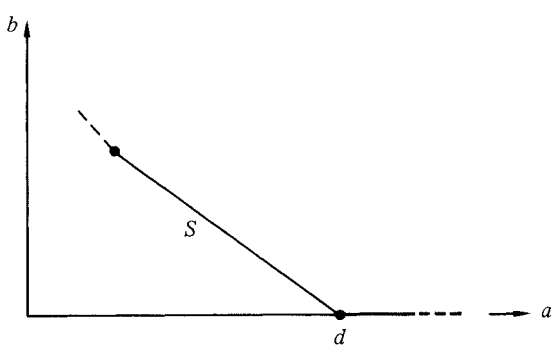

where the segment S touching the a-axis at $(a, b)=(d, 0)$ has slope $-(q-1)/q$. Indeed, this would be implied by the fact that the first Newton-Puiseux pair

is $(q, q-1)$, except for the possibility of an unessential initial Newton-Puiseux pair $(1, p)$ or $(p, 1)$. An initial Newton-Puiseux pair $(p, 1)$ with $p>1$ would be essential in the diagram Γ, and would thus give the wrong diagrams Γ and Ω, so it cannot occur. If the first pair were $(1, p)$ with $p \geqq 1$, the subsequent Newton-Puiseux pair (s, t) would have to satisfy $t/s > p$. In particular, it could not be $(q, q-1)$, so it would also have to be inessential, namely $(1, p')$ say with $p' > p$, and we can repeat *ad absurdem.*

Consider the part $g_0(x, z)$ of $g(x, z)$ given by the monomials whose exponents (a, b) are on the segment S, that is, they satisfy $(q-1)a+qb=(q-1)d$. If one takes out the largest factor x^s occurring in $g_0(x, z)$, the result is homogeneous in x^q and $z^{(q-1)}$ and can thus be factored into factors of the form $x^q - a z^{(q-1)}$. Thus $g(x, z)$ has the form

$$g(x, z) = x^s \prod_v (x^q - \alpha_v z^{(q-1)})^{r_v} + \sum e_{ab} x^a z^b,$$

where $d = s + q\sum_v r_v = s + qr$ and the sum is over (a, b) with $(q-1)a+qb > (q-1)d$ and $a+b \leqq d$. Thus

$$h(x, y, z) = x^s \prod_v (x^q - a_v y z^{(q-1)})^{r_v} + \sum e_{ab} x^a y^{d-a-b} z^b,$$

and

$$f(x, y) = x^s \prod_v (x^q - a_v y)^{r_v} + \sum e_{ab} x^a y^{d-a-b}.$$

The exponents $(i, j) = (a, d-a-b)$ in the sum satisfy $qj + i = qd - (q-1)a - qb < d$, as desired. □

We have thus shown that some minimal RPI diagram can be realized by an embedding $\mathbb{C}^2 \subset \mathbb{P}^2$. The proof that *any* minimal RPI diagram for $\mathscr{L}$ can be so realized is similar and we just sketch it. We assume that we have already chosen an embedding $\mathbb{C}^2 \subset \mathbb{P}^2$ that gives a minimal RPI diagram Ω for $\mathscr{L}$. Suppose that Ω' is another minimal RPI diagram for $\mathscr{L}$ which differs from Ω in that the root node has been moved past a single "contributing node," in the terminology of Theorem 6.2. The analysis of Sect. 6 shows that we can get from any minimal RPI diagram for $\mathscr{L}$ to any other by a sequence of such steps, so it suffices to show that Ω' is realizable.

The situation is as follows (omitted edge weights are 1):

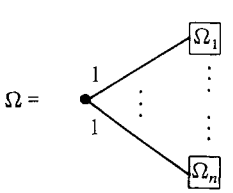

with

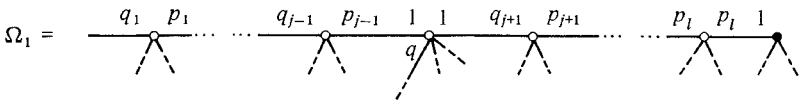

where, if we label the shown vertices $v_1, \ldots, v_{l+1}$, then v_j is the contributing node in question and v_{l+1} is the root node for Ω' (it may not actually be a vertex of Ω, since it may have valency 2). The splice diagram of the singularity of $\bar{V} \cup \mathbb{P}^1$ at the point at infinity corresponding to Ω_1 is

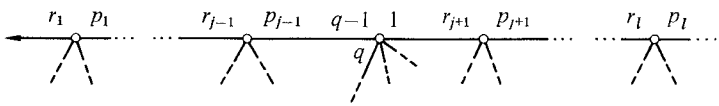

(with $r_i = p_i - q_i$ for $i = 1, \ldots, j-1$ and $r_i = q^2 p_i - q_i$ for $i = j+1, \ldots, l-1$).

We again make a linear change of coordinates to put the point at infinity that we are looking at $x=0$ and then again the equation $g(x, z)=0$ for $\bar{V}$ at this point at infinity can be analyzed by its Newton polygon, which will have the form

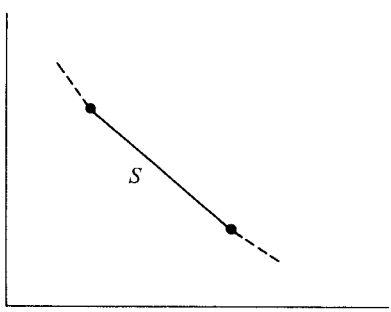

where S is a segment of slope $-(q-1)/q$. (The segments below S will have slopes $-r_i/p_i$ for $i=1, \ldots, j-1$, while the segments above S have slopes depending on what, if anything, is beyond the q-weighted edge out of the vertex v_j.) It follows that $g(x, z)$ has the form

$$g(x,z) = \prod_{\nu=1}^{k} (x^q - a_\nu z^{(q-1)})^{r_\nu} \prod_{\mu=1}^{k'} (x^{\alpha_\mu} - b_\mu z^{\beta_\mu})^{\rho_\mu} + \sum e_{ab} x^a z^b,$$

where the $-\beta_\mu/\alpha_\mu$ are the slopes of the segments other than S of the Newton polygon boundary (possibly with repetitions) and the sum involves only monomials whose exponents pairs are strictly inside the Newton polygon. k is the number of 1-weighted edges at the contributing node v_j. The factors in the products are the one-Newton-Puiseux-pair approximations to the branches of $\bar{V}$ at the point in question; the first product corresponds to the branches whose first Newton-Puiseux pair is the $(q, 1)$ coming from the node v_j. In particular,

we may assume that the r_1-fold factor $(x^q - a_1 z^{(q-1)})^{r_1}$ approximates the branches that correspond to the part of Ω_1 to the right of the contributing node v_j. In (x, y) coordinates this approximating curve is $(x^q - a_1 y)$. If we make the change of coordinates $(x, y) \mapsto \left(x, y + \frac{1}{a_1} x^q\right)$, we obtain a new RPI splice diagram in which this first $(q, 1)$ Newton-Puiseux pair at infinity for these particular branches has been cancelled, while the other factors $(x^q - a_v y)$ still have the same form (with changed constant a_v). Thus the root node has been moved to the right of the contributing node v_j. This new splice diagram may not be Ω', since it may now have an initial inessential Newton-Puiseux pair $(q', 1)$ (with $q' < q$), but the first part of this proof can then be used to reduce to a minimal RPI diagram again. This final diagram will be Ω' since only the first Newton-Puiseux pair is affected by the above coordinate changes, so the root node cannot move past any other contributing vertex during the above process. □

8. Discussion and examples

Our results give an effective computational tool: it is a finite problem to compute the possible realizations of a given link as a link at infinity since the degree of the realizing polynomial is determined by the splice diagram, and if one prescribes the topology for an algebraic plane curve one generally gets a small set of possible splice diagrams. A general manifestation of this latter statement is the following finiteness result.

Proposition 8.1. *There are only finitely many regular toral links with a given number of components and with given genus (= genus of a minimal Seifert surface) if one excludes links having a regular splice diagram with root vertex of valency $n = 2$ and such that neither edge adjacent to the root has positive far weight.*

Proof. By Corollary 5.3 it suffices to show that for any bound N there are, up to isotopy, only finitely many multilinks $\mathscr{L}$ satisfying:

(i) $\mathscr{L}$ has a minimal multilink RPI diagram Ω satisfying the condition of Proposition 5.4 (all l_v are positive) and either with root vertex u of valency $n \neq 2$ or with a node u adjacent to the root vertex and having positive far weight;

(ii) $|\chi(F)| \leqq N$, where F is a fiber of the multilink.

Theorem 11.1 of [E-N] says

$$\chi(F) = \sum_{v \in \Omega^\circ} (2 - \delta_v) l_v. \tag{8.1}$$

If w is a leaf and v is the adjacent node then $l_v = a_v l_w$. In this case let $l'_v = (\alpha_v - 1) l_w$. If v has no adjacent leaf let $l'_v = l_v$. Let u be as above, and if $n = 1$ let u' be

the node next to u and otherwise $u'=u$. By rewriting Eq. (8.1) as a sum over nodes one sees

$$|\chi(F)\geqq l'_u+\sum_{v\in\Omega^*-\{u'\}} l'_v. \tag{8.2}$$

Thus $|\chi(F)|$ is at least the number of nodes of Ω, so the number of nodes is bounded. Moreover l'_u is bounded, and it bounds the number of arrowheads, so there are only finitely many possibilities for the shape of Ω. Moreover, l'_u clearly bounds (α_v-1) for every node v, so the near weights are all bounded. Now fix a shape of Ω and fix the near weights. Then for any node v, l'_v is positive and bounded, and this clearly implies upper and lower bounds on the far weight β_v at v. Thus there are only finitely many possibilities for Ω. □

Corollary 8.2. *If there are infinitely many regular plane curves $V\subset\mathbb{C}^2$ up to proper isotopy with given genus g and number m of components at infinity then $m\geqq 2$ and all but finitely many of them are given (up to an algebraic automorphism of $\mathbb{C}^2$) by equations of the form $f(x,y)=0$ where $f(x,y)=x^p y^q+f_0$ with $p,q>0$ and f_0 only involving monomials $x^a y^b$ with $a\leqq p$, $b\leqq q$, $(a,b)\neq(p,q)$.*

Proof. The proof is an easy Newton polygon computation; we describe it in greater generality then we need now, since we need the same approach later. Let Ω be the splice diagram for a reduced curve V with exactly two points at infinity. By a linear transformation we may put these points at $x=0$ and $y=0$. Then the defining polynomial for V may be taken to be

$$f(x,y)=x^p y^q+\sum_{a+b<p+q} c_{ab}\,x^a y^b.$$

Now let N_1 be the convex hull in $\mathbb{R}^2$ of the set of exponent pairs (a,b) occurring in f together with the "point" $(0,-\infty)$ and the part of the line $a+b=p+q$ below the point (p,q). Denote the finite segments of its boundary by $S_1,\ldots,S_k$.

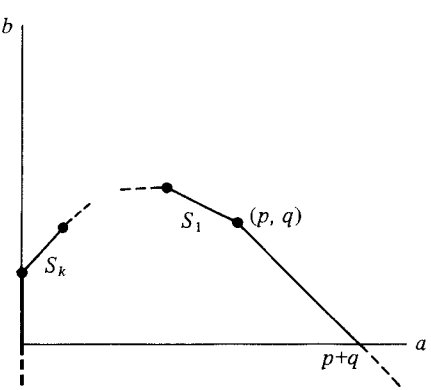

(8.3)

The defining polynomial for $\bar{V}\subset\mathbb{P}^2=\mathbb{C}^2\cup\mathbb{P}^1$ in a neighborhood of the point $x=z=0$ at infinity is

$$g(x,z)=x^p+\sum c_{ab}\,x^a z^{p+q-a-b}.$$

Thus the Newton polygon N for g at this point is just the image of N_1 under the transformation $(a, b) \mapsto (a, p+q-a-b)$. We can therefore use the slopes of the finite segments of ∂N_1 instead of ∂N to compute the initial Newton-Puiseux pairs of the branches of $\bar{V}$ at the point $x=z=0$, and hence part of the splice diagram Ω. The answer is that (an initial approximation to) Ω has the form:

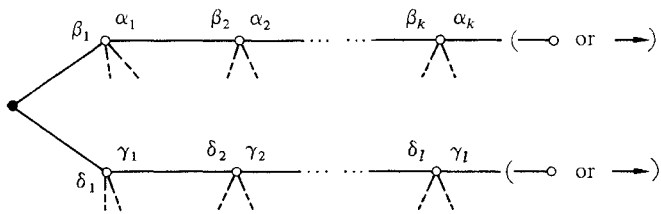

(8.4)

where, in the top row, $-\beta_i/\alpha_i$ is the slope of the segment S_i of ∂N_1, and the final vertex is a leaf or arrowhead according as segment S_k touches the b-axis or not (the data in the bottom row are computed similarly from the polygon N_2 obtained by reversing the roles of a and b). This is only an initial approximation to Ω in that it may not be a minimal splice diagram: the pair (α_k, β_k) will be inessential if S_k touches the b-axis and $\alpha_k = 1$; similarly for (γ_l, δ_l).

Now suppose there exists an exponent pair (a, b) with $b > q$. Then segment S_1 would have negative slope and β_1 would be positive. Moreover, the slope of S_1 is strictly between 0 and -1, so it cannot be an integer, so $\alpha_1 > 1$, so the pair (α_1, β_1) is essential. Similarly if some (a, b) has $a > p$ then $\delta_1 > 0$. The corollary thus follows from Proposition 8.1. □

Before we give explicit examples, we mention a corollary of work of Abhyankar and Moh which can simplify non-realizability computations. Let

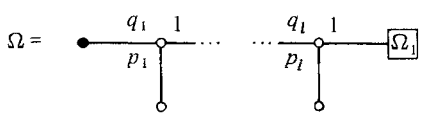

be an RPI splice diagram, all of whose arrowheads are in Ω_1, and put

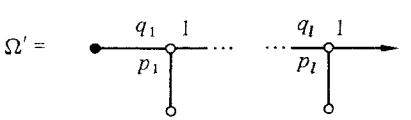

Proposition 8.3. *If Ω can be realized by a link at infinity then so can Ω'.*

Proof. A realization $f(x, y) = 0$ of Ω will have degree $P = p_1 \ldots p_l q$ for some q. We can assume it meets infinity at $x=0$, and $f(x, y) = x^P + (\text{lower order})$. Let

$g(x, z)=0$ be the defining equation in coordinates at the point $x=z=0$ at infinity, obtained by homogenizing f and then putting $y=1$. The main result of [A-M 1] says in our language that if $g_0(x, z)$ is the approximate q-th root of g (in the sense that $g-g_0^q$ has degree less than $p_1 \ldots p_l(q-1)$ in x), then the singularity at $(x, z)=(0, 0)$ of $g_0(x, z)=0$ realizes the splice diagram at infinity corresponding to Ω'. Let $f_0(x, y)$ be the corresponding polynomial in x, y coordinates. Since $f_0(x, y)=0$ has just the one point $x=0$ at infinity, it realizes Ω'. □

Low genus examples

We describe reduced curves $V \subset \mathbb{C}^2$ of low genus whose links $\mathscr{L}$ at infinity are knots (this classification can also be done using Abhyankar's methods: [A] and [A-S]). As already mentioned, such a V is always regular at infinity, so $\mathscr{L}$ will be a regular toral knot. A regular toral knot is a knot $\mathscr{L}=\mathcal{O}\{p_1, q_1; p_2, q_2; \ldots; p_k, q_k\}$ obtained by iterated cabling from the unknot $\mathcal{O}$, with cabling coefficients $p_i>1$, $q_i>0$ satisfying $gcd(p_i, q_i)=1$, $1<q_1<p_1$, and $q_i<p_i p_{i-1} q_{i-1}$ for $i>1$. If this $\mathscr{L}$ is the link at infinity of V then (possibly after an algebraic automorphism of $\mathbb{C}^2$), V is given by a polynomial of degree $P=p_1 \ldots p_k$ and has genus (by Theorem 4.2):

$$g(V)=\tfrac{1}{2}\left(\sum_1^k (q_i(p_i-1)p_{i+1} \ldots p_k)-P+1\right).$$

The table lists the regular toral knots up to genus 4. For each one, the most general polynomial (up to algebraic automorphisms of the domain $\mathbb{C}^2$ and affine transformations of the range $\mathbb{C}$) realizing $\mathscr{L}$ as a regular link at infinity is also listed if it exists. This list is easily continued, but the computations of the polynomials become tedious, as the example $f_3(x, y)$ of the table suggests.

$\mathscr{L}$	P	g	f
$\mathcal{O}$	1	0	x
$\mathcal{O}\{3, 2\}$	3	1	x^3+y^2+ax
$\mathcal{O}\{5, 2\}$	5	2	$x^5+y^2+ax^3+bx^2+cx$
$\mathcal{O}\{3, 2; 2, 1\}$	6	2	–
$\mathcal{O}\{4, 3\}$	4	3	$x^4+y^3+y(ax^2+bx+c)+dx^2+ex$
$\mathcal{O}\{3, 2; 2, 3\}$	6	3	$f_1(x, y)$
$\mathcal{O}\{7, 2\}$	7	3	$x^7+y^2+ax^5+bx^4+cx^3+dx^2+ex$
$\mathcal{O}\{3, 2; 3, 1\}$	9	3	–
$\mathcal{O}\{5, 3\}$	5	4	$x^5+y^3+y(ax^3+bx^2+cx+d)+ex^3+fx^2+gx$
$\mathcal{O}\{3, 2; 2, 5\}$	6	4	$f_2(x, y)$
$\mathcal{O}\{9, 2\}$	9	4	$x^9+y^2+ax^7+bx^6+cx^5+dx^4+ex^3+fx^2+gx$
$\mathcal{O}\{3, 2; 3, 2\}$	9	4	$f_3(x, y)$
$\mathcal{O}\{5, 2; 2, 1\}$	10	4	–
$\mathcal{O}\{3, 2; 4, 1\}$	12	4	–
$\mathcal{O}\{3, 2; 2, 1; 2, 1\}$	12	4	–

where

$$f_1(x,y)=(x^3+y^2)^2+ax^4+bx^3+\tfrac{1}{4}a^2x^2+cx$$
$$+axy^2+by^2+dy, \quad (d\neq 0),$$

$$f_2(x,y)=(x^3+y^2)^2+ax^4+bx^3+cx^2+dx$$
$$+axy^2+by^2+exy+fy, \quad (e\neq 0),$$

$$f_3(x,y)=(x^3+y^2)^3+3ax^7+bx^6+3a^2x^5+2abx^4+cx^3$$
$$+a^2bx^2+dx+6ax^4y^2+2bx^3y^2+3a^2x^2y^2+2abxy^2$$
$$+(c-a^3)y^2-6axy^4+by^4, \quad (d\neq a^4-8ac).$$

Thus, in each case the most general curve with the given link at infinity is given by $f(x,y)=h$, where h is an additional constant. Note that if any one of the parameters $a, b, \ldots h$ is non-zero, then it can be made equal to 1 by a further linear transformation, so the true number of parameters in each case is one less than appears.

The method of computation is as follows. We can assume that we have realized the minimal RPI splice diagram, so our realization is in degree $P=p_1\ldots p_k$. We can also assume the point at infinity is at $x=0$. As in the previous section, there are no initial inessential Newton-Puiseux pairs at infinity, so the defining polynomial has the form:

$$f(x,y)=(x^{p_1}-ay^{q_1})^{p/p_1}+\sum c_{ij}x^iy^j,$$

sum over monomials with $i+j\leqq P$ and $q_1i+p_1j<Pq_1$. A linear change of coordinates makes $\alpha=-1$ and a further change of coordinates of the form $(x,y)\mapsto(x+c, y+t(x))$ with $\deg(t)<p_1/q_1$ will eliminate several monomials, simplifying subsequent computation. Now, working with the polynomial $g(x,z)$ at infinity, compute the conditions on the coefficients c_{ij} implied by the values of the further Newton-Puiseux pairs, keeping in mind that there may be intervening inessential pairs. (The Newton-Puiseux pairs for the singularity at infinity are the pairs $(p_i, q_i'=p_1^2\ldots p_{i-1}^2p_i-q_i)$ occurring in the splice diagram at infinity; between (p_i, q_i') and (p_{i+1}, q_{i+1}') there can be inessential pairs $(1,k_1), (1,k_2), \ldots$, with $p_iq_i'<k_1<k_2<\ldots<q_{i+1}'/p_{i+1}$.) The computed conditions express some coefficients c_{ij} in terms of "earlier" ones. By iteratively satisfying them, the general form for the polynomial f is eventually reached.

Such results can also be used to classify singular curves. For instance, an algebraic embedding V of $\mathbb{C}$ in $\mathbb{C}^2$ with one node is connected at infinity, so its defining polynomial is good, and a nearby fiber will be a once punctured torus (it picks up an extra homology class: the vanishing cycle of the node). By the above table, the defining polynomial is $f(x,y)=x^3+y^2+ax$ and V is given by $f(x,y)=b$, for some a and b. If $a=0$ then the only singular fiber is $f(x,y)=0$, which has a cusp, not a node. Thus $a\neq 0$ and a linear change of coordinates puts f in the form $f(x,y)=c_1(x^3-y^2+x^2)+c_2$, for some constants c_1 and c_2. The only singular fiber is now at $f=c_2$, so V is described by $y^2=x^3+x^2$.

Regular algebraic annuli

Using the estimates in the proof of Proposition 8.1 one sees that a minimal regular splice diagram Ω for a two component link $\mathscr{L}$ of genus 0 must have root vertex of valency 2 and $l_v=0$ for every node v. By Corollary 5.2, every node is adjacent to the root vertex. It follows that Ω is one of the diagrams:

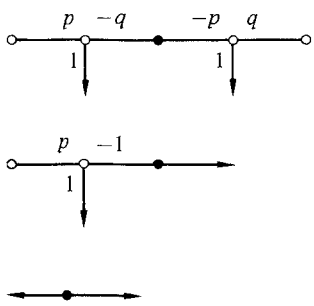

We now apply the calculation in the proof of Corollary 8.2. Assume f is as in that proof. By considering linking of the virtual component S_{root} with the two components of $\mathscr{L}$ one sees that the p and q occurring in f agree with the p and q in the splice diagram (recall that S_{root} is the link at infinity of a generic line). Since the link at infinity has only one component near $x=0$ and one near $y=0$, each of the polygons N_1 and N_2 has just one finite segment in its boundary, connecting the point (p, q) to the b-axis or a-axis respectively. Inessential Newton-Puiseux pairs may occur but by a change of coordinates $(x, y)\mapsto(x-a, y-b)$ we can eliminate any $(1, 0)$ pair. The slope of the boundary segment S_1 of N_1 is then positive and bounded by q/p so it cannot be integral (unless $p=q=1$), so inessential Newton-Puiseux pairs can only occur at the $y=0$ component. Changing to coordinates (y, z) near the point $y=z=0$ at infinity, one can now eliminate inessential pairs one by one by coordinate transformations to see that the polynomial at infinity has the form (up to linear change of coordinates)

$$g(y, z)=(y+a_{r-1}z^2+\ldots+a_0 z^{r+1})^q-z^{p+q}$$

with $rq<p$. We thus have:

Proposition 8.4. *Up to algebraic automorphisms, a regular curve $V\subset\mathbb{C}^2$ which is topologically an open annulus is given by an equation of the form $f(x, y)=1$ with*

$$f(x, y)=x^p y^q, \quad \text{or}$$

$$f(x, y)=(y x^r+a_{r-1}x^{r-1}+\ldots+a_0)^q x^{p-rq}$$

with $0<q\leqq p$, $0<rq>p$, $a_0\neq 0$, and p and q coprime. □

The fiber $f^{-1}(0)$ is the only irregular fiber for f. Its link at infinity has splice diagram

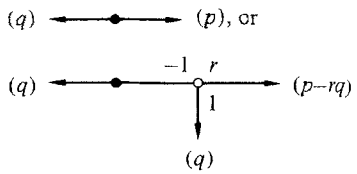

respectively. The former diagram is also the diagram for the multilink associated with $\mathscr{L}$.

Irregular algebraic annuli

These exist also. Let p, q, r be positive integers with p and r coprime and $r>1$, $p<(q+1)r$. Consider $f(x, y)=(x^q y+1)^r+x^p$. Then $V=f^{-1}(0)$ is smooth, and the splice diagram Ω for its link $\mathscr{L}$ at infinity is

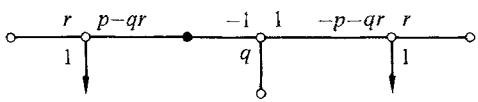

Theorem 4.3 shows that the euler characteristic of V is 0, and since V has no closed components, it must be either an annulus or the disjoint union of a punctured sphere and a punctured torus. The latter possibility is ruled out because the two components have non-trivial linking number. Thus V is an annulus. This f has another irregular fiber, $f^{-1}(1)$, whose link at infinity has splice diagram

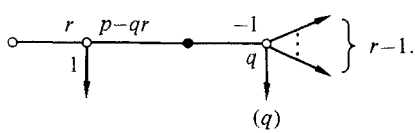

The regular link at infinity for f has splice diagram

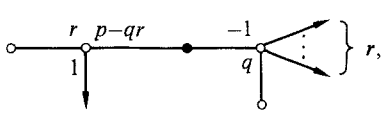

so Theorem 4.3 implies that a regular fiber of f has euler characteristic $p(1-r)$ and hence topological genus $(p-1)(r-1)/2$.

Two points at infinity

We make two comments about the setup in the proof of 8.2 which are useful in computations. Firstly, let v_i denote the i-th vertex in the top row of the RPI diagram (8.4). Then:

Proposition 8.5. *$(\delta_{v_i}-2)l_{v_i}$ equals the oriented area of the parallelogram spanned by the vectors from the origin to the beginning and end points of segment S_i (see (8.3)).*

We will not use this proposition, so we just sketch a proof: the proposition is true by direct calculation for the simplest polynomial with the appropriate Newton polynomial N_1 and deforming such a polynomial to any other polynomial with the same N_1 does not change the relevant linking numbers. □

The second comment is that the edge determinant $\beta_1\delta_1-\alpha_1\gamma_1$ of the "root edge" that results by suppressing the root node in (8.4) is non-positive. Indeed, draw both N_1 and N_2 on the same diagram:

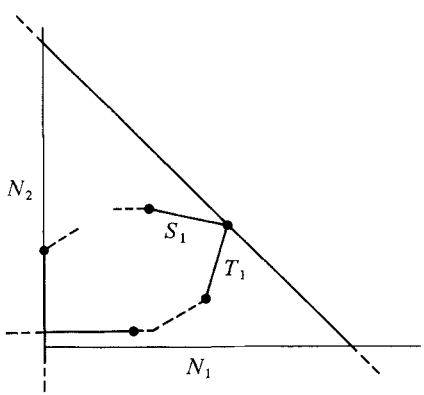

Now $-\beta_1/\alpha_1$ is the slope of the segment S_1 of ∂N_1 and $-\gamma_1/\delta_1$ is the slope of the corresponding segment T_1 of ∂N_2 and the non-positivity of $\beta_1\delta_1-\alpha_1\gamma_1$ is equivalent to the fact that the angle from S_1 to T_1 is in the interval $[0,\pi)$. However, the RPI diagram (8.4) may not be minimal. We shall show that the non-positivity of this edge determinant persists when one eliminates inessential Newton-Puiseux pairs. This gives the following result, which was an ingredient in the proof of Theorem 6.5 (and hence also in Theorem 3 in the irregular case).

Proposition 8.6. *If a reduced curve has 2 points at infinity, Ω is the minimal* RPI *splice diagram for its link at infinity, and Ω_0 is the splice diagram that results by suppressing the root vertex of Ω, then the root edge (and hence every edge) of Ω_0 has non-positive edge determinant.*

Proof. We must show that eliminating inessential Newton-Puiseux pairs next to the root vertex cannot cause trouble. Note that an inessential pair $(1, 0)$ can be eliminated by a linear transformation, so we may assume it doesn't

occur. If (α_1, β_1) is inessential (i.e. $\alpha_1 = 1$) then segment S_1 has integral slope $-\beta_1$ and touches the b-axis. Moreover, its slope is in the interval $(0, q/p]$. Similarly, if (γ_1, δ_1) is inessential then the integer $-\delta_1$ is in the interval $(0, p/q]$. Thus if both are inessential then $p=q$ and $f(x, y)$ only involves monomials of the form $x^i y^i$. The proposition is easily verified in this case. Thus we may assume that only one pair is inessential, say $(\gamma_1, \delta_1)=(1, \delta)$.

This inessential pair occurs at the point $y=0$ at infinity, so we homogenize f and put $x=1$ to get the equation $g(y, z)=0$ at infinity. g results from f by replacing each monomial $x^a y^b$ in f by $y^b z^{p+q-a-b}$, so the Newton polygon N_2' for g is the image of N_2 under the transformation $(a, b) \mapsto (b, p+q-a-b)$. Let N_1' be the image of N_1 under this transformation. All exponent pairs (a, b) occurring in f lie in the domain $N_1 \cap N_2$, so all exponent pairs (i, j) occurring in g lie in $N_1' \cap N_2'$. We picture this below; S_i' is the image of S_i and T_1' is the image of T_1.

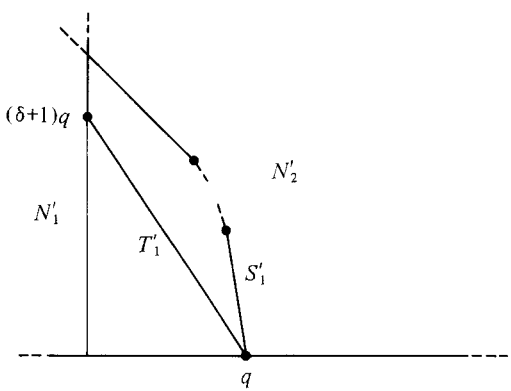

The non-positivity of the relevant edge determinant is equivalent to the fact that the angle from S_1' to T_1' is non-negative.

Now g has the form, for some constant a,

$$g(y, z)=(y+az^{\delta+1})^q+\sum d_{ij} y^i z^j,$$

sum over monomials satisfying $(\delta+1)i+j>(\delta+1)q$. Replace $g(y, z)$ by $g_1(y, z) = g(y-az^{\delta+1}, z)$ to eliminate the inessential Newton-Puiseux pair. The monomials of g_1 all have exponent pairs on segments of slope $-(\delta+1)$ above points (i, j) of $N_1' \cap N_2'$, so S_1' is still in the boundary of a convex domain which contains these exponent pairs. Thus if T_1'' is the segment at $(q, 0)$ of the boundary new Newton diagram N_2'', then the angle from S_1' to T_1'' is still non-negative. Since the slope of T_1'' gives the next Newton-Puiseux pair at infinity, the new edge determinant is still non-positive. If this Newton-Puiseux pair is also inessential we can iterate the argument. Thus the proof is complete. □

9. Problems

A main question is to determine to what extent the results of this paper can be extended to irregular curves $V \subset \mathbb{C}^2$. Note that the link at infinity $\mathscr{L}$ of such a V may be a multilink, since V may have multiple components. In this case the existence of nontrivial multiplicities in $\mathscr{L}$ makes clear that V is irregular. Conjecturally, the fact that a curve $V \subset \mathbb{C}^2$ is irregular at infinity can always be read off from its link at infinity: if V is reduced, the link at infinity should not be a regular toral link (we make a more specific conjecture below). Conjecturally also, the link at infinity determines the topology of $V \subset \mathbb{C}^2$ to the extent possible—namely the topology of the least singular V with the given link. An optimal result would be that for any given multilink $\mathscr{L}$, the set of all curves with $\mathscr{L}$ as link at infinity is a connected semi-algebraic set. In particular, $\mathscr{L}$ would determine the topology of the generic member $V \subset \mathbb{C}^2$ of this set.

Note that there are two different degrees of irregularity at infinity:

(i) A fiber $f^{-1}(c)$ may be irregular at infinity because it has multiple components but nevertheless have all sufficiently large spheres around the origin transverse to all nearby fibers. This should maybe be considered to be still regular at infinity: the results of this paper can for the most part be generalized to cover this case by allowing multilinks in the discussion.

(ii) A fiber $f^{-1}(c)$ is "truly irregular at infinity" if there is no ε such that large spheres are transverse to all fibers $f^{-1}(z)$ with $|z-c|<\varepsilon$.

The following specific conjecture would imply that the multilink at infinity of *any* plane curve V, regular or not, determines the link at infinity $\mathscr{L}_0$ of a regular fiber V_0 of the defining polynomial for V, and hence determines the topology of such a regular fiber. Recall that $\mathscr{L}_0$ is determined by and determines a certain multilink $\mathscr{L}'$ (Theorems 4 and 5).

Conjecture. *The link at infinity of a plane curve V (reduced or not) is truly irregular at infinity if and only if its* RPI *(multilink) splice diagram Ω is irregular—that is, some l_v is negative (multiplicities should be taken into account in computing l_v). Moreover, the multilink $\mathscr{L}'$ associated to the link at infinity of a regular fiber of the defining polynomial is determined as follows: for each node v with $l_v<0$ such that all nodes w between v and the root vertex have $l_w \geqq 0$, delete the portion of Ω beyond v (viewed from the root vertex) and replace v by an arrowhead with the unique multiplicity that leaves l_w unchanged for vertices w closer to the root vertex than v.*

The proof of Proposition 8.3 implies a very weak form of part of this conjecture: if Ω is as in that proposition then the portion Ω' of Ω agrees with the corresponding portion of the RPI splice diagram for any other fiber of the defining polynomial $f(x, y)$ for V, and hence also agrees with the corresponding portion of the diagram for the multilink. The reason is that $f_0(x, y)$ of the proof of 8.3 is unchanged if one replaces $f(x, y)$ by $f(x, y)-c$.

Even for regular links at infinity many problems remain, the most obvious of which is to give a closed form characterization among regular toral links of those that can be realized as regular links at infinity. Another question that

arose during this study, but which is much less central, is whether the vanishing of the "enhancement to the Milnor number" $\lambda(\mathscr{L})$ (see [R], [N-R 1]) characterizes regular toral links among fibered RPI toral links. It is immediate from the computation in [N-R 2] of $\lambda(\mathscr{L})$ for fibered toral links $\mathscr{L}$ that $\lambda(\mathscr{L})$ vanishes if $\mathscr{L}$ is regular.

References

[A] Abhyankar, S.S.: On Expansion techniques in algebraic geometry. Tata Institute of Fundamental Research. Lect. Math. Phys. **57**, 1977

[A-M 1] Abhyankar, S.S., Moh, T.T.: Newton-Puiseux expansion and generalized Tschirnhausen transformation. I. J. Reine Angew. Math. **260**, 47–83 (1973)

[A-M 2] Abhyankar, S.S., Moh, T.T.: Embeddings of the line in the plane. J. Reine Angew. Math. **276**, 148–166 (1975)

[A-S] Abhyankar, S.S., Singh, B.: Embeddings of certain curves. Am. J. Math. **100**, 99–175 (1978)

[E-N] Eisenbud, D., Neumann, W.: Three-Dimensional link theory and invariants of plane curve singularities. Ann. Math. Stud. **101**, Princeton: University Press 1985

[J] Johannson, K.: Homotopy equivalences of 3-manifolds with boundaries. Lect. Notes Math. vol 761. New York Berlin Heidelberg: Springer 1979

[J–S] Jaco, W., Shalen, P.: Seifert fibered spaces in 3-manifolds. Memoirs of the A.M.S. **220**, 1979

[M] Milnor, J.: Singular points of complex hypersurfaces. Ann. Math. Stud. **61**, Princeton: University Press, 1968

[N-R 1] Neumann, W.D., Rudolph, L.: Unfoldings in knot theory. Math. Ann. **278**, 409–439 (1987) and: Corrigendum: Unfoldings in knot theory. ibid. **282**, 349–351 (1988)

[N-R 2] Neumann, W.D., Rudolph, L.: Difference index of vectorfields and the enhanced Milnor number. Topology (to appear)

[R] Rudolph, L.: Isolated critical points of maps from $\mathbb{R}^4$ to $\mathbb{R}^2$ and a natural splitting of the Milnor number of a classical fibered link. Part I. Comm. Math. Helv. **62**, 630–645 (1987)

[S] Suzuki, M.: Propriétés topologiques des polynômes de deux variables complexes, et automorphismes algébriques de l'espace $\mathbb{C}^2$. J. Math. Soc. Jpn. **26**, 241–257 (1974)

[Z-L] Zaidenberg, M.G., Lin, V.Y.: An irreducible, simply connected curve in $\mathbb{C}^2$ is equivalent to a quasihomogeneous curve. (English translation) Soviet Math. Dokl. **28**, 200–204 (1983)

[W] Waldhausen, F.: On irreducible 3-manifolds that are sufficiently large. Ann. Math. **87**, 56–88 (1968)

Oblatum 28-XII-1988 & 11-IV-1989